

## Validation of MIPAS-ENVISAT H<sub>2</sub>O operational data collected between July 2002 and March 2004

G. Wetzel, Hermann Oelhaf, Gwenaël Berthet, A. Bracher, C Cornacchia, D.  
G. Feist, H Fischer, A. Fix, M. Iarlori, A. Kleinert, et al.

► **To cite this version:**

G. Wetzel, Hermann Oelhaf, Gwenaël Berthet, A. Bracher, C Cornacchia, et al.. Validation of MIPAS-ENVISAT H<sub>2</sub>O operational data collected between July 2002 and March 2004. Atmospheric Chemistry and Physics, European Geosciences Union, 2013, 13, pp.5791 - 5811. 10.5194/acp-13-5791-2013 . insu-01109482

**HAL Id: insu-01109482**

**<https://hal-insu.archives-ouvertes.fr/insu-01109482>**

Submitted on 26 Jan 2015

**HAL** is a multi-disciplinary open access archive for the deposit and dissemination of scientific research documents, whether they are published or not. The documents may come from teaching and research institutions in France or abroad, or from public or private research centers.

L'archive ouverte pluridisciplinaire **HAL**, est destinée au dépôt et à la diffusion de documents scientifiques de niveau recherche, publiés ou non, émanant des établissements d'enseignement et de recherche français ou étrangers, des laboratoires publics ou privés.



## Validation of MIPAS-ENVISAT H<sub>2</sub>O operational data collected between July 2002 and March 2004

G. Wetzel<sup>1</sup>, H. Oelhaf<sup>1</sup>, G. Berthet<sup>2</sup>, A. Bracher<sup>3,\*</sup>, C. Cornacchia<sup>4</sup>, D. G. Feist<sup>5</sup>, H. Fischer<sup>1</sup>, A. Fix<sup>6</sup>, M. Iarlori<sup>7</sup>, A. Kleinert<sup>1</sup>, A. Lengel<sup>1,\*\*</sup>, M. Milz<sup>8</sup>, L. Mona<sup>4</sup>, S. C. Müller<sup>9,\*\*\*</sup>, J. Ovarlez<sup>2</sup>, G. Pappalardo<sup>4</sup>, C. Piccolo<sup>10,\*\*\*\*</sup>, P. Raspollini<sup>10</sup>, J.-B. Renard<sup>2</sup>, V. Rizi<sup>7</sup>, S. Rohs<sup>11,\*\*\*\*\*</sup>, C. Schiller<sup>11,†</sup>, G. Stiller<sup>1</sup>, M. Weber<sup>3</sup>, and G. Zhang<sup>1</sup>

<sup>1</sup>Institute for Meteorology and Climate Research (IMK), Karlsruhe Institute of Technology (KIT), Karlsruhe, Germany

<sup>2</sup>Laboratoire de Physique et Chimie de l'Environnement et de l'Espace (LPC2E), CNRS, Orléans, France

<sup>3</sup>Institute of Environmental Physics and Remote Sensing (IUP/IFE), University of Bremen, Bremen, Germany

<sup>4</sup>CNR-IMAA, Consiglio Nazionale delle Ricerche – Istituto di Metodologie per l'Analisi Ambientale, Tito Scalo, Potenza, Italy

<sup>5</sup>Max Planck Institute for Biogeochemistry, Jena, Germany

<sup>6</sup>Deutsches Zentrum für Luft- und Raumfahrt (DLR), Institut für Physik der Atmosphäre, Oberpfaffenhofen, Germany

<sup>7</sup>CETEMPS – Dipartimento di Scienze Fisiche e Chimiche – Università degli Studi, L'Aquila, Italy

<sup>8</sup>Department of Computer science, Electrical and Space engineering, Luleå University of Technology, Kiruna, Sweden

<sup>9</sup>Institute of Applied Physics (IAP), University of Bern, Bern, Switzerland

<sup>10</sup>Istituto di Fisica Applicata “Nello Carrara” (IFAC), del Consiglio Nazionale delle Ricerche (CNR), Firenze, Italy

<sup>11</sup>Institute for Energy and Climate Research – Stratosphere (IEK-7), Forschungszentrum Jülich, Jülich, Germany

\* now at: Alfred Wegener Institute (AWI), Bremerhaven, Germany

\*\* now at: Carl Zeiss AG, Oberkochen, Germany

\*\*\* now at: METEOTEST, Bern, Switzerland

\*\*\*\* now at: Met Office, Exeter, UK

\*\*\*\*\* now at: Institute for Energy and Climate Research – Troposphere (IEK-8), Forschungszentrum Jülich, Jülich, Germany

† deceased

Correspondence to: G. Wetzel (gerald.wetzel@kit.edu)

Received: 11 January 2013 – Published in Atmos. Chem. Phys. Discuss.: 15 February 2013

Revised: 16 May 2013 – Accepted: 20 May 2013 – Published: 14 June 2013

**Abstract.** Water vapour (H<sub>2</sub>O) is one of the operationally retrieved key species of the Michelson Interferometer for Passive Atmospheric Sounding (MIPAS) instrument aboard the Environmental Satellite (ENVISAT) which was launched into its sun-synchronous orbit on 1 March 2002 and operated until April 2012. Within the MIPAS validation activities, independent observations from balloons, aircraft, satellites, and ground-based stations have been compared to European Space Agency (ESA) version 4.61 operational H<sub>2</sub>O data comprising the time period from July 2002 until March 2004 where MIPAS measured with full spectral resolution. No significant bias in the MIPAS H<sub>2</sub>O data is seen in the lower stratosphere (above the hygropause) between about 15 and 30 km. Differences of H<sub>2</sub>O quantities observed by

MIPAS and the validation instruments are mostly well within the combined total errors in this altitude region. In the upper stratosphere (above about 30 km), a tendency towards a small positive bias (up to about 10%) is present in the MIPAS data when compared to its balloon-borne counterpart MIPAS-B, to the satellite instruments HALOE (Halogen Occultation Experiment) and ACE-FTS (Atmospheric Chemistry Experiment, Fourier Transform Spectrometer), and to the millimeter-wave airborne sensor AMSOS (Airborne Microwave Stratospheric Observing System). In the mesosphere the situation is unclear due to the occurrence of different biases when comparing HALOE and ACE-FTS data. Pronounced deviations between MIPAS and the correlative instruments occur in the lowermost stratosphere and

upper troposphere, a region where retrievals of H<sub>2</sub>O are most challenging. Altogether it can be concluded that MIPAS H<sub>2</sub>O profiles yield valuable information on the vertical distribution of H<sub>2</sub>O in the stratosphere with an overall accuracy of about 10 to 30 % and a precision of typically 5 to 15 % – well within the predicted error budget, showing that these global and continuous data are very valuable for scientific studies. However, in the region around the tropopause retrieved MIPAS H<sub>2</sub>O profiles are less reliable, suffering from a number of obstacles such as retrieval boundary and cloud effects, sharp vertical discontinuities, and frequent horizontal gradients in both temperature and H<sub>2</sub>O volume mixing ratio (VMR). Some profiles are characterized by retrieval instabilities.

## 1 Introduction

Water vapour (H<sub>2</sub>O) is a highly variable atmospheric constituent. It plays a dominant role in the transfer of energy in the atmosphere. While it is a strong greenhouse gas in the troposphere, its emission in the infrared spectral region contributes to a cooling in the stratosphere. Hence, the H<sub>2</sub>O amount in the upper troposphere and lowermost stratosphere (UT/LS) has a considerable effect on the outgoing long-wave radiation which regulates the global radiation budget of the atmosphere (see, e.g. Forster and Shine, 1999; Solomon et al. 2010).

Water vapour is produced in the troposphere mainly by evaporation processes over water and land surfaces leading to maximum concentrations near the Earth's surface which decrease strongly with altitude. H<sub>2</sub>O enters the stratosphere primarily in the tropics through the tropical transition layer (TTL) (see, e.g. Brasseur and Solomon, 2005). However, the actual pathways of water transport from the UT into the lower stratosphere are still under debate (see, e.g. Fueglistaler et al., 2009). In the stratosphere, mixing ratios are increasing with altitude due to methane oxidation. The competing H<sub>2</sub>O loss reaction with the electronically excited oxygen atom (producing the OH radical) becomes only important in the upper stratosphere and lower mesosphere and yields, along with shortwave photodissociation reactions, to declining H<sub>2</sub>O values in the mesosphere and thermosphere. Recent research has focused on a positive global trend in stratospheric H<sub>2</sub>O mixing ratios over the 1980s and 1990s (e.g. Michelsen et al., 2000; Oltmans et al., 2000; Rosenlof et al., 2001; Nedoluha et al., 2003) whereas a substantial and unexpected decrease in stratospheric water was documented after the year 2000 (Randel et al., 2006; Scherer et al., 2008; Fueglistaler, 2012). Understanding trends in H<sub>2</sub>O in the radiatively sensitive UT/LS along with the underlying processes is crucial for understanding and predicting rates of global warming (Solomon et al., 2010).

Satellite measurements are essential for monitoring the distribution and trend of H<sub>2</sub>O on a global scale. One of the first spaceborne instruments able to measure stratospheric H<sub>2</sub>O was the Limb Infrared Monitor of the Stratosphere (LIMS) (Fischer et al., 1981; Russell III et al., 1984), a limb-emission filter radiometer which was deployed aboard the Nimbus-7 satellite launched in October 1978. In the 1980s and 1990s the Atmospheric Trace Molecule Spectroscopy instrument (ATMOS) as the first limb occultation Fourier transform infrared (FTIR) spectrometer provided H<sub>2</sub>O profiles from the upper troposphere to the lower mesosphere during four short missions of the Space Shuttle between 1985 and 1994 (Abbas et al., 1996a, b). The second Stratospheric Aerosol and Gas Experiment (SAGE II) was launched into its orbit in October 1984 and provided a 21 yr record of global trace gas measurements of the sunlit upper troposphere and stratosphere using solar occultation in the visible and near-infrared spectral region (Chiou et al., 1997). Further H<sub>2</sub>O measurements were obtained in the visible spectral range by the Halogen Occultation Experiment (HALOE) aboard the Upper Atmosphere Research Satellite (UARS) between 1991 and 2005 (Harries et al., 1996; Nedoluha et al., 2003). Other instruments on UARS detecting H<sub>2</sub>O have been the Improved Stratospheric and Mesospheric Sounder (ISAMS) (Goss-Custard et al., 1996) and the Microwave Limb Sounder (MLS) (Pumphrey et al., 2000). The Cryogenic Infrared Spectrometers and Telescopes for the Atmosphere (CRISTA) experiment performed limb emission H<sub>2</sub>O measurements with high spatial resolution during two missions of the Space Shuttle in 1994 and 1997 (Offermann et al., 2002).

More recently, solar occultation satellite instruments observing H<sub>2</sub>O in the stratosphere were the Polar Ozone and Aerosol Measurement (POAM) III instrument (Nedoluha et al., 2003; Lumpe et al., 2006) and the Improved Limb Atmospheric Sounder (ILAS/ILAS-II) (Kanzawa et al., 2003; Griesfeller et al., 2008).

Spaceborne instruments which are still in operation and which measure vertical profiles of H<sub>2</sub>O are the Sub-Millimeter Radiometer (SMR) aboard the Odin satellite (Urban et al., 2007), launched in February 2001; the Atmospheric Chemistry Experiment Fourier Transform Spectrometer (ACE-FTS) on the SCISAT-1 satellite (Nassar et al., 2007; Carleer et al., 2008), launched in August 2003; a second-generation MLS on the Aura satellite (Manney et al., 2005; Santee et al., 2005) with data from begin of mission in August 2004.

The Michelson Interferometer for Passive Atmospheric Sounding (MIPAS; Fischer et al., 2008) is one of the three chemistry instruments onboard ENVISAT, besides the Scanning Imaging Absorption Spectrometer for Atmospheric Chartography (SCIAMACHY; Bovensmann et al., 1999) and the Global Ozone Monitoring by Occultation of Stars (GOMOS) instrument (Bertaux et al., 1991). It measures a

wide range of tracers, chemically active species and climate relevant constituents including H<sub>2</sub>O.

The complexity and lifetime of such space instruments along with the importance of H<sub>2</sub>O demand large efforts in validation. Balloon-borne observations are very useful for validation, being capable of measuring accurately a large number of molecules with a large vertical coverage at superior vertical resolution. Since the number of balloon flights is limited special care has to be taken concerning the quality of the coincidence. This holds also for aircraft measurements (e.g. Falcon and Learjet) which may cover larger horizontal regions compared to balloons but from distinctly lower flight altitudes. Ground-based measurements can be carried out more or less continuously, but the information on the vertical distribution of H<sub>2</sub>O is mostly limited to the troposphere and lower stratosphere. The use of independent satellite measurements for validation purposes has the great advantage that nearly global coverage in combination with a large statistics for all seasons is available.

This paper outlines the results of the MIPAS H<sub>2</sub>O validation activities for the operational H<sub>2</sub>O products of version 4.61 provided by the European Space Agency (ESA). It belongs to a series of validation studies of MIPAS operational products which were performed in a consistent manner: temperature (Ridolfi et al., 2007), O<sub>3</sub> (Cortesi et al., 2007), HNO<sub>3</sub> (Wang et al., 2007), CH<sub>4</sub>, N<sub>2</sub>O (Payan et al., 2009), and NO<sub>2</sub> (Wetzel et al., 2007). In accordance with these validation studies, the H<sub>2</sub>O assessment is restricted to the time period from July 2002 until March 2004 where MIPAS was operated at full spectral resolution. H<sub>2</sub>O profile comparisons between version 4.61 and the newly processed ML2PP\_V6 data (Raspollini et al., 2013) have shown that differences in retrieved H<sub>2</sub>O volume mixing ratios are less than 5% in the stratosphere except in the Antarctic winter where differences can be around 10% or larger.

In the following section, an overview of the MIPAS data analysis is given. Section 3 describes the intercomparison method and the comparison to different validation instruments and another retrieval processor. Section 4 gives concluding remarks for MIPAS H<sub>2</sub>O data users.

## 2 MIPAS operations and H<sub>2</sub>O data

The limb-viewing Fourier transform spectrometer MIPAS on ENVISAT (MIPAS-E) has been designed to operate in the mid-infrared spectral region covering five spectral bands between 685 and 2410 cm<sup>-1</sup> with an unapodized full spectral resolution of 0.025 cm<sup>-1</sup> (Fischer et al., 2008). The vertical instantaneous field of view (IFOV) is about 3 km. The instrument was launched into its sun-synchronous orbit by ESA on 1 March 2002. It passes the Equator in a southwards direction 14.3 times each day at 10:00 local time. After the commissioning phase MIPAS was run predominantly in its nominal measurement mode from July 2002 until the end of March

2004. During each orbit approximately 72 limb scans covering tangent altitudes between 8 and 68 km were recorded (in steps of 3 km below 45 km) in the full spectral resolution mode. The validation of H<sub>2</sub>O based on this data and time period is the subject of this paper.

After an increasing frequency of problems with the interferometer drive system in late 2003 and beginning of 2004 and upon subsequent detailed investigations it was decided to suspend the nominal operations from March 2004 onwards for detailed investigations. From January 2005 to April 2012 (when the communication with the satellite platform was lost) the instrument was back to operation but at reduced spectral resolution (41% of nominal) for the benefit of an equivalent improvement in spatial sampling. The duty cycle of this so-called optimized resolution mode has been steadily increasing from 30% in January 2005 to 100% from December 2007 on. The different spectral and spatial sampling of MIPAS since 2005 has posed changes in the calibration scheme and the processing codes. Although the validation of this new reduced spectral resolution mode data is not finished yet and is therefore not included in this paper, there is so far no indication of any significant deterioration in the quality of the H<sub>2</sub>O data.

Level 1b and level 2 processing of data version 4.61 (high spectral resolution mode) including all steps from raw data to calibrated spectra and profiles of atmospheric parameters has been performed by ESA using the operational processors described by Kleinert et al. (2007) for level 1b and Raspollini et al. (2006) for level 2. Calibrated spectra are analysed using a global fit approach by varying the input parameters of the forward model according to a non-linear Gauss–Newton procedure. Since the retrieval is performed on the same vertical grid as the measurements and the inversion process has been found to be sufficiently well conditioned, regularization and a priori information appeared not necessary for a stable retrieval. In a first step, temperature and pressure at the measured tangent altitudes are retrieved simultaneously. In the next steps, volume mixing ratio (VMR) profiles of the primary target species H<sub>2</sub>O, O<sub>3</sub>, HNO<sub>3</sub>, CH<sub>4</sub>, N<sub>2</sub>O, and NO<sub>2</sub> are retrieved individually in the reported sequence.

The H<sub>2</sub>O operational version 4.61 data analysis has been carried out in the following four microwindows: 807.850–808.450, 946.650–947.700, 1645.525–1646.200, and 1650.025–1653.025 cm<sup>-1</sup>. A random retrieval error due to instrument noise is extracted from the diagonal elements of the error variance covariance matrix calculated during the retrieval process. Further error sources are estimated for day and night conditions and different seasons. The following parameter errors and forward model errors have been taken into account for the H<sub>2</sub>O profile retrieval: pressure/temperature random retrieval errors; spectroscopic data errors due to uncertainties in the intensity, width and position of emission lines; radiometric gain, instrumental line shape, and spectral calibration inaccuracies; uncertainties in assumed profiles of the contaminant species O<sub>3</sub>, ClONO<sub>2</sub>, and NH<sub>3</sub>; uncertainty

in high-altitude H<sub>2</sub>O column above the uppermost retrieval level; horizontal gradient effects due to assuming a horizontally homogeneous atmosphere for each profile; and errors due to the assumption of local thermodynamic equilibrium (LTE) in the upper atmosphere (above 45 km). Pressure/temperature and spectroscopic data errors are the dominant error sources in the stratosphere and upper troposphere. The random error ranges typically between 5 and 25 % in this altitude region while the total error is within 10 to 30 %. The total error is calculated as the root mean square of random and systematic components. A detailed discussion of all error components together with their magnitudes is given in Raspollini et al. (2006).

### 3 Intercomparison results

In the following sections, H<sub>2</sub>O profiles observed by airborne and satellite sensors as well as H<sub>2</sub>O observations from ground and H<sub>2</sub>O radiosonde data are compared to MIPAS version 4.61 H<sub>2</sub>O data with a coincidence criterion of 300 km and 3 h (if not otherwise specified). Pressure is used as the primary vertical coordinate and the MIPAS averaging kernel is applied to the correlative data in case of significant differences in altitude resolution according to the method described in Rodgers (2000). All differences between measured quantities of MIPAS and the validation instrument are expressed in either absolute units or as relative differences. The mean difference  $\Delta x_{\text{mean}}$  for  $N$  profile pairs of compared observations is given as

$$\Delta x_{\text{mean}} = \frac{1}{N} \sum_{n=1}^N (x_{M,n} - x_{I,n}), \quad (1)$$

where  $x_M$  and  $x_I$  are VMR values of MIPAS and the validating instrument at one altitude level. The mean relative difference  $\Delta x_{\text{mean,rel}}$  of a number of profile pairs is calculated by dividing the mean absolute difference by the mean profile value of the validation instrument (reference instrument):

$$\Delta x_{\text{mean,rel}} = \frac{\Delta x_{\text{mean}}}{\frac{1}{N} \sum_{n=1}^N x_{I,n}} \cdot 100 \%. \quad (2)$$

Differences are displayed together with the combined errors  $\sigma_{\text{comb}}$  of both instruments which are defined as

$$\sigma_{\text{comb}} = \sqrt{\sigma_M^2 + \sigma_I^2}, \quad (3)$$

where  $\sigma_M$  and  $\sigma_I$  are the precision, systematic or total errors of MIPAS and the validation instrument, respectively. Precision errors characterize the reproducibility of a measurement and correspond, in general, to random noise errors. For statistical comparisons, systematic errors of the temperature profile used for the H<sub>2</sub>O retrievals behave randomly and are therefore included in the precision (random) part of the error

budget. Other error sources are treated as systematic. This approach was applied to all validation studies of MIPAS operational trace gas products as a matter of consistency (Cortesi et al., 2007; Payan et al., 2009; Wang et al., 2007; Wetzel et al., 2007). It should be mentioned that not all error sources (as specified in Sect. 2) could be characterized for all validation instruments in the same detail. However, dominant error sources (e.g. spectroscopic uncertainties) have been included. The uncertainty of the calculated mean difference (standard error of the mean, SEM) is given by  $\sigma/N^{0.5}$  where  $\sigma$  is the standard deviation (SD). The comparison between the standard deviation of the mean difference and the combined random error helps to validate the precision of MIPAS since both terms should be of comparable magnitude. A bias between MIPAS and another instrument is considered significant if the standard error of the bias (SEM) is smaller than the bias itself. The comparison between the VMR difference of MIPAS versus the correlative instruments and the combined systematic error in the case of statistical comparisons or total error in the case of single comparisons is appropriate to identify unexplained biases in the MIPAS H<sub>2</sub>O observations when they exceed these combined error limits.

#### 3.1 Intercomparison of balloon-borne observations

As part of the validation program of the chemistry instruments aboard ENVISAT a number of balloon flights carrying in situ and remote sensing instruments were performed within dedicated campaigns at various geophysical conditions. An overview of all balloon flights used for H<sub>2</sub>O validation is given in Table 1.

Three validation flights were carried out within 2002 to 2004 with the cryogenic Fourier transform infrared spectrometer MIPAS-B, the balloon-borne version of MIPAS, covering midlatitude summer, polar winter/spring, and polar summer conditions. The flights took place from Aire sur l'Adour (France, 44° N) on 24 September 2002, Kiruna (Sweden, 68° N) on 20/21 March 2003, and again from Kiruna on 3 July 2003. MIPAS-B can be regarded as precursor of MIPAS on ENVISAT. Therefore, a number of specifications are quite similar, such as spectral resolution and spectral coverage. For some critical parameters, however, the MIPAS-B performance is superior, e.g. in the case of the NESR (noise equivalent spectral radiance), and in the case of the pointing accuracy and precision which is, in terms of tangent altitude, in the order of 90 m ( $3\sigma$ ). Further improvement of the NESR can be achieved by averaging spectra taken at the same pointing angle which is justified in the balloon case. MIPAS-B measures all atmospheric parameters covered by MIPAS-E. Essential for the balloon instrument is the sophisticated line of sight stabilization system, which is based on an inertial navigation system and supplemented with an additional star reference system. The MIPAS-B data processing including instrument characterization is described in Friedl-Vallon et al. (2004) and references

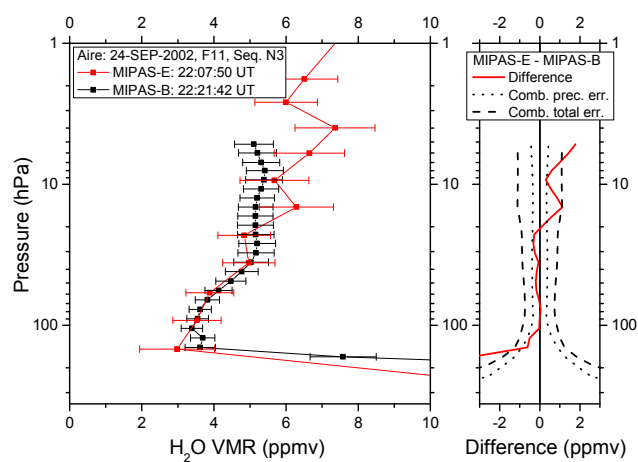
**Table 1.** Overview of balloon flights used for the validation of MIPAS-E. Distances and times between MIPAS-E and the validation instrument refer to an altitude of 20 km.

Location	Date	Instrument	Distance	Time difference
Kiruna (Sweden, 68° N)	16 Jan 2003	ELHYSA	532 km	183 min
	06 Mar 2003	FISH	192 km	73 min
	20/21 Mar 2003	MIPAS-B	78/28 km	15/24 min
	09 Jun 2003	FISH	312 km	1 min
	03 Jul 2003	MIPAS-B	2 km	501 min
	11 Mar 2004	ELHYSA	195 km	28 min
Aire sur l'Adour (France, 44° N)	24 Sep 2002	MIPAS-B	207/79 km	14/10 min

therein. The measurements were done typically at a 1.5 km grid. Retrieval calculations of atmospheric target parameters were performed at a 1 km grid with a least squares fitting algorithm using analytical derivative spectra calculated by the Karlsruhe Optimized and Precise Radiative transfer Algorithm (KOPRA; Stiller et al., 2002; Höpfner et al., 2002). A Tikhonov–Phillips regularization approach constraining with respect to the shape of an a priori profile was adopted. The resulting vertical resolution is typically between 2 and 4 km for the H<sub>2</sub>O retrieval and is therefore comparable to or better than the vertical resolution of MIPAS-E. H<sub>2</sub>O was analysed in MIPAS-B proven microwindows in the  $\nu_2$  band centred at 1595 cm<sup>-1</sup>. Transitions between 1210 and 1245 cm<sup>-1</sup> and around 808 and 825 cm<sup>-1</sup> have also been used for the data analysis. Spectroscopic parameters chosen for the MIPAS-B retrieval are consistent with the database taken for the MIPAS-E data analysis (Flaud et al., 2003) and originate mainly from the HITRAN 2004 database (Rothman et al., 2005). A further overview on the MIPAS-B data analysis is given in Wetzel et al. (2006) and references therein.

A perfect coincidence between MIPAS-B and MIPAS-E could be achieved during the flight on 24 September 2002 above southern France. The mean distance of both observations in the compared altitude region was within about 200 km and the mean time difference was not more than 14 min. The MIPAS-E profile (see Fig. 1) is in good agreement with MIPAS-B between about 20 and 100 hPa. Above these altitudes, MIPAS-E exhibits higher H<sub>2</sub>O values. This positive bias turns out to be significant with respect to the combined total errors above about 7 hPa indicating possible yet unidentified systematic errors there. A negative bias is visible around and below the hygropause. The altitude of the hygropause is captured very well by MIPAS-E. Some retrieval instabilities which occur frequently in the ESA operational data retrieval are also visible.

A summary of all MIPAS balloon comparisons to MIPAS-E H<sub>2</sub>O is depicted in Fig. 2. For most altitudes, any deviation is within the combined error limits. A positive bias is visible above about 20 hPa. Large deviations occur around the hygropause and below where the H<sub>2</sub>O mixing ratios strongly increase. However, the mean difference lies clearly within the combined total error, except at the lower-

**Fig. 1.** Comparison of H<sub>2</sub>O profiles (left panel) measured by MIPAS-B (flight no. 11, sequence N3, black squared line) and MIPAS-E (orbit 2975, red squared line) on 24 September 2002 above southern France along with difference (right panel, red solid line), 1 $\sigma$  combined precision (black dotted lines) and total errors (black dashed lines). Line styles are shown in the figure legend.

most altitude region below about 200 hPa. The mean difference above 200 hPa pressure altitude (averaged over all altitudes) amounts to 0.13 ppmv (parts per million by volume) or 3.0 %.

As a further test we compare also the hydrogen budget. The oxidation chain of the molecule CH<sub>4</sub> produces about two molecules of H<sub>2</sub>O in the stratosphere. The sum  $H = [H_2O] + 2[CH_4]$  is therefore a good measure for the hydrogen budget because it is a quasi-conserved quantity in this altitude region. Figure 3 displays the hydrogen budget as obtained by both MIPAS instruments in comparison to earlier in situ observations (Engel et al., 1996; Herman et al., 2002). In general, MIPAS-E individual mixing ratio profiles exhibit larger variations (at least partly caused by retrieval oscillations) compared to the profiles retrieved from MIPAS-B spectra. Mean inferred mixing ratio profiles of both MIPAS instruments are within the range of the in situ measurements at around 7 ppmv. Between 120 and 7 hPa, deviations between mean MIPAS-E and MIPAS-B profiles are

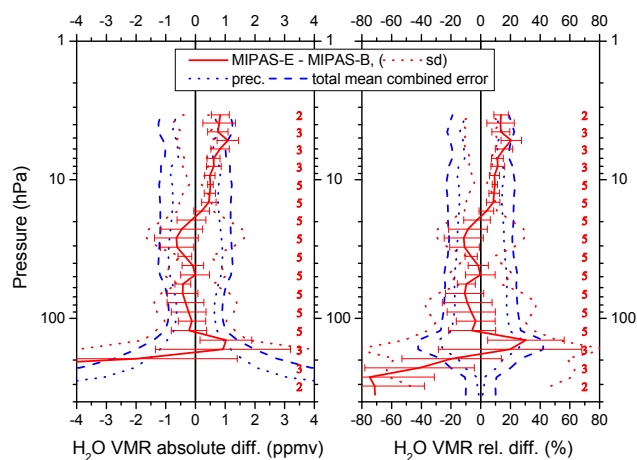


**Fig. 2.** Mean absolute and relative differences of all comparisons between MIPAS-E and MIPAS-B (red solid lines) including standard deviation (red dotted lines) and the standard error of the mean, plotted as error bars around the mean deviation together with precision (blue dotted lines) and total (blue dashed lines) mean combined errors. Red values (along the right-hand y-axes) indicate the number of collocations used for the statistical analysis at corresponding pressure levels.

small. Mean deviations above and below this altitude region are mostly within the combined total errors. The shape of the mean H difference profile is similar to the mean difference H<sub>2</sub>O profile shown in Fig. 2, since the hydrogen budget is dominated by the molecule H<sub>2</sub>O and mean CH<sub>4</sub> deviations between both sensors are less than 0.4 ppmv in all compared altitudes (Payan et al., 2009).

The frost point hygrometer ELHYSA (Etude de L'Hygrométrie Stratospherique) was developed at the LMD (Laboratoire de Météorologie Dynamique) and has been operated routinely from balloon and airborne platforms since 1987; it is now operated by LPC2E (Laboratoire de Physique et Chimie de l'Environnement et de l'Espace). The stratospheric balloon version acquires real-time in situ H<sub>2</sub>O profiles from the upper troposphere and the lower stratosphere (see, e.g. Ovarlez and Ovarlez, 1994) with a vertical resolution of few tens of metres and with a high absolute accuracy of several percent.

ENVISAT validation flights with ELHYSA were performed on 16 January 2003 and 11 March 2004 from Kiruna. Results are displayed in Fig. 4. The in situ ELHYSA profile was smoothed with the averaging kernel of MIPAS. The overall agreement between MIPAS and ELHYSA is satisfactory for both flights. However, some deviations occur in the lowermost stratosphere near 100 hPa and in the upper troposphere near 300 hPa (January flight). Anyhow, differences are mostly within the combined errors.

The Fast In situ Stratospheric Hygrometer (FISH) has been developed at the Forschungszentrum Jülich and is based on the Lyman- $\alpha$  photofragment fluorescence technique. FISH

has been used in several campaigns both from balloon and aircraft. With a measurement frequency of 1 Hz, the noise equivalent mixing ratio at 3 ppmv is 0.13–0.18 ppmv, and the accuracy is 0.15–0.2 ppmv. Further details of the instrument and the calibration procedure are described in Zöger et al. (1999).

Data of two balloon flights have been used for the inter-comparison with MIPAS. Both flights were performed from Kiruna on 6 March 2003 and 9 June 2003, respectively. Figure 5 shows H<sub>2</sub>O profiles measured during the FISH flight onboard the TRIPLE balloon gondola on 6 March 2003. The MIPAS profile exhibits some retrieval instabilities yielding to differences which are barely within the combined total error limits. However, the mean difference between MIPAS and the smoothed FISH profile is only  $-0.16$  ppmv ( $-2.7\%$ ). For the June 2003 flight, the comparison was restricted to only three altitude levels due to a lack of FISH data between about 20 and 60 hPa. To increase the small number of matches between MIPAS-E and FISH, 4-days forward and backward trajectories have been calculated using a coincidence criterion of 150 km and 0.5 h. The trajectory model (McKenna et al., 2002) uses operational analyses of the European Centre for Medium-Range Weather Forecasts (ECMWF) on a  $1^\circ \times 1^\circ$  latitude/longitude grid. Figure 6 displays mean differences between MIPAS-E and FISH for this trajectory comparison. Only collocations below about 50 hPa pressure altitude could be found for comparison. In this altitude range, mean differences are less than 1 ppmv (20 %) and within the combined total errors. It is noticeable that for the upper two altitudes, where statistics is enhanced, the agreement with MIPAS-E is close to perfect. However, standard deviations are generally larger than the combined precision errors.

A summary of the direct comparison of all balloon flights is given in Fig. 7. A mean difference profile was calculated taking into account the number of coincident measurement sequences. Below about 13 km at mid and high latitudes, the mean difference of all inter-comparisons is quite large. This can presumably be explained by uncertainties regarding the exact altitude of the tropopause and hygropause in connection with the strong H<sub>2</sub>O gradient in the troposphere, as well as due to sometimes strong horizontal inhomogeneities and cloud effects. Above this altitude region, mean deviations are mostly well inside the combined errors. It should be mentioned that the pronounced deviation between FISH and MIPAS-E at 24 km is linked to only one single collocation. The overall standard deviation is largely comparable to the combined precision errors. Above about 27 km, MIPAS-E H<sub>2</sub>O values reveal a slight positive bias increasing with altitude. Anyhow, the mean deviation over all altitudes above 10 km is found to be only 0.07 ppmv (1.7 %). Hence the general agreement between balloon-borne observations and MIPAS-E is found to be quite good.

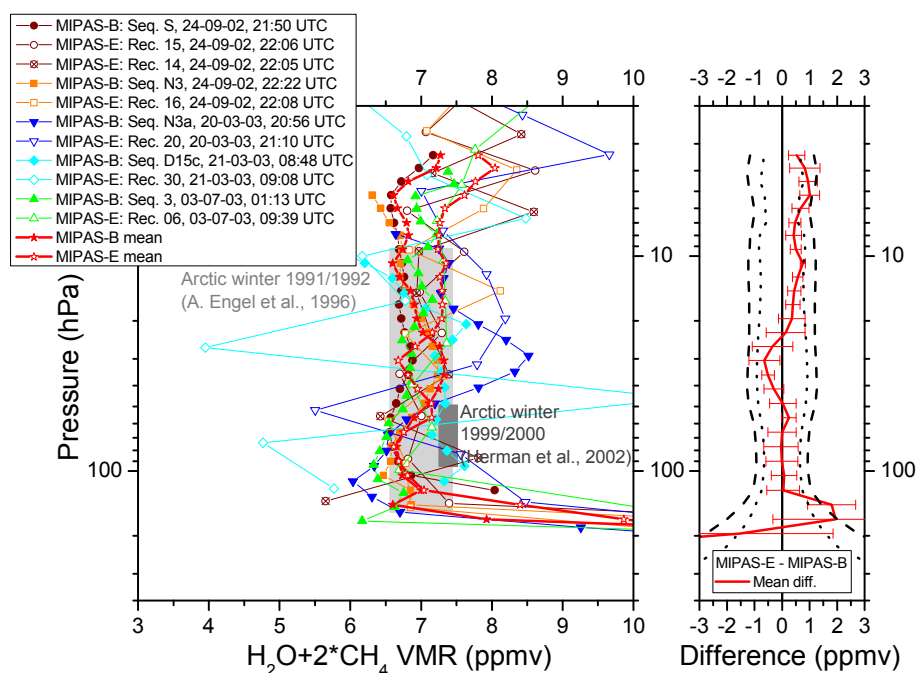


**Fig. 3.** Hydrogen budget of all comparisons between MIPAS-E and MIPAS-B (left panel) together with absolute differences (right panel) and combined precision (dotted lines) and total errors (dashed lines). For comparison, Arctic winter balloon-borne observations (solid grey bar) performed by Engel et al. (1996) and aircraft measurements (solid dark grey bar) carried out by Herman et al. (2002) are also shown.

**Table 2.** Overview on aircraft flights used for the validation of MIPAS-E. Distances between MIPAS-E and the validation instrument refer to the UT/LS region.

Instrument	Date	Lat. range	Orbit	Distance	Time difference
FISH (aboard Geophysica)	18 Jul 2002	35–46° N	2001	≤ 300 km	≤ 3 h
	22 Jul 2002		2051		
	24 Oct 2002		3403		
	15 Jan 2003	61–78° N	4585	≤ 300 km	≤ 3 h
	19 Jan 2003		4649		
	08 Feb 2003		4935		
	28 Feb 2003		5214		
	02 Mar 2003		5250		
	12 Mar 2003		5386/5387		
H <sub>2</sub> O-DIAL (aboard Falcon)	18 Oct 2002	38–50° N	3318	<80 km	<2 h
	23 Oct 2002		3390		
	24 Oct 2002		3404		
	25 Oct 2002		3411		
AMSOS (aboard Swiss Air Force Learjet)	17 Sep 2002	16–89° N	2865–2868	≤ 300 km	≤ 3 h
	18 Sep 2002		2881		
	19 Sep 2002		2896		

### 3.2 Intercomparison of aircraft observations

The validation programme of the chemistry instruments aboard ENVISAT comprised also a number of aircraft flights where H<sub>2</sub>O was measured in situ and with remote sensing

instruments within dedicated campaigns. An overview of aircraft flights used for H<sub>2</sub>O validation is given in Table 2.

The hygrometer (FISH) has already been described in Sect. 3.1. An aircraft version was flown several times aboard the high-altitude M55 Geophysica aircraft. MIPAS validation flights were performed from Forli (Italy) and Kiruna



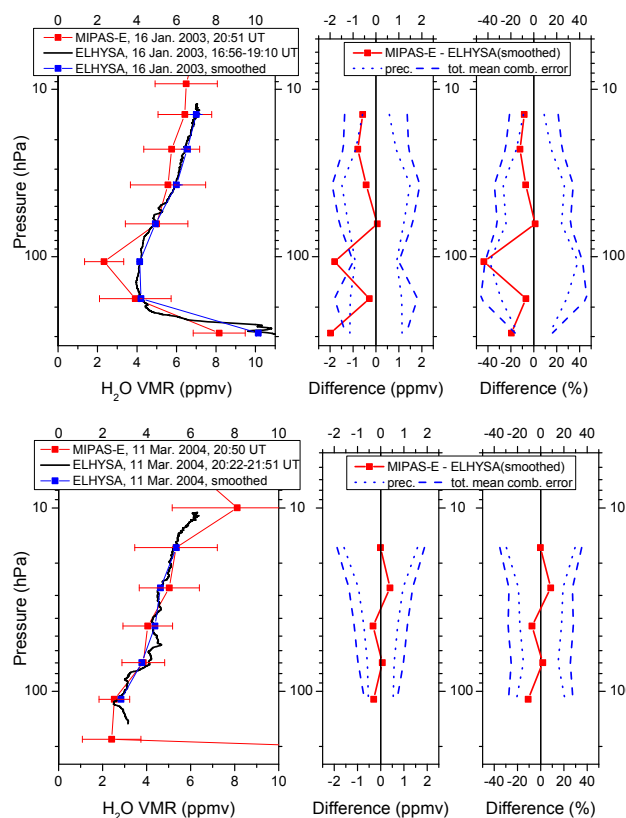


**Fig. 4.** Comparison between MIPAS-E (red squared line) and ELHYSA (black solid line) measured H<sub>2</sub>O profiles from 16 January 2003 (top) and 11 March 2004 (bottom) at Kiruna (~68° N) along with absolute and relative differences (blue squared lines) and combined errors (blue dotted and dashed lines). The in situ ELHYSA profile was smoothed with the averaging kernel of MIPAS-E (blue squared line) to make the vertical resolution of both instruments comparable.

(Sweden) between July 2002 and March 2003. Figures 8 and 9 show mean differences between MIPAS and FISH for all Geophysica flights within a 300 km and 3 h coincidence limit in direct coincidence (Fig. 8) and with 4-days forward and backward trajectory calculations (McKenna et al., 2002) looking for matches between MIPAS and FISH within a coincidence criterion of 150 km and 0.5 h (Fig. 9). The direct coincidence comparison exhibits a significant negative deviation of MIPAS with respect to (smoothed) FISH in the upper troposphere and lowermost stratosphere of up to 75 % at 180 hPa. However, when taking into account the increasing number of coincidences in the trajectory match, the deviations decrease to less than 10 %, which is clearly within the combined systematic error limits. This example illustrates the problem of validation of H<sub>2</sub>O in regions with very high spatial variability.

The DLR airborne water vapour Differential Absorption Lidar (H<sub>2</sub>O-DIAL) was flown onboard the Falcon aircraft several times from Forli in October 2002. A system descrip-

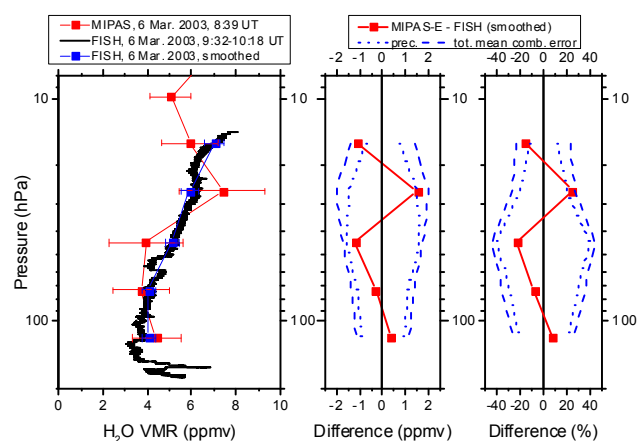


**Fig. 5.** Direct comparison of H<sub>2</sub>O profiles measured by MIPAS-E and the balloon-borne in situ instrument FISH on 6 March 2003 at Kiruna (~68° N) along with absolute and relative differences and combined errors. The in situ FISH profile was smoothed with the averaging kernel of MIPAS-E to make the vertical resolution of both instruments comparable. Annotation as per Fig. 4.

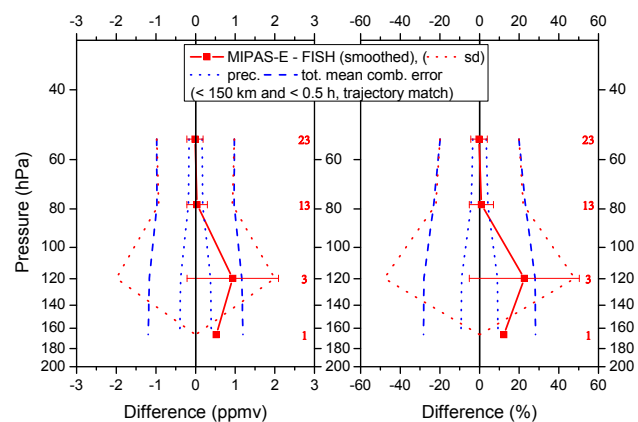


**Fig. 6.** Mean differences from a trajectory match statistics between H<sub>2</sub>O profiles measured by MIPAS-E and balloon-borne FISH on 6 March 2003 and 9 June 2003 together with combined errors, as well as standard deviation and the standard error of the mean, plotted as error bars. Annotation as per Fig. 2.

tion together with an assessment of accuracy is given by Poberaj et al. (2002) and Kiemle et al. (2008). Individual results of the comparison to MIPAS observations around Italy are shown in Fig. 10. Although in general not more than two MIPAS data points of the vertical profile overlap with the DIAL profile observations, the DIAL has a much higher resolution than MIPAS in the tropopause region and is thus well adapted to validate MIPAS data in this region where water vapour is difficult to measure due to strong gradients. In addition, clouds that may affect the MIPAS retrieval can clearly be detected with the DIAL. Since spatial and temporal collocation was good for all cases, and no clouds were detected above the flight path of the aircraft, MIPAS data are most

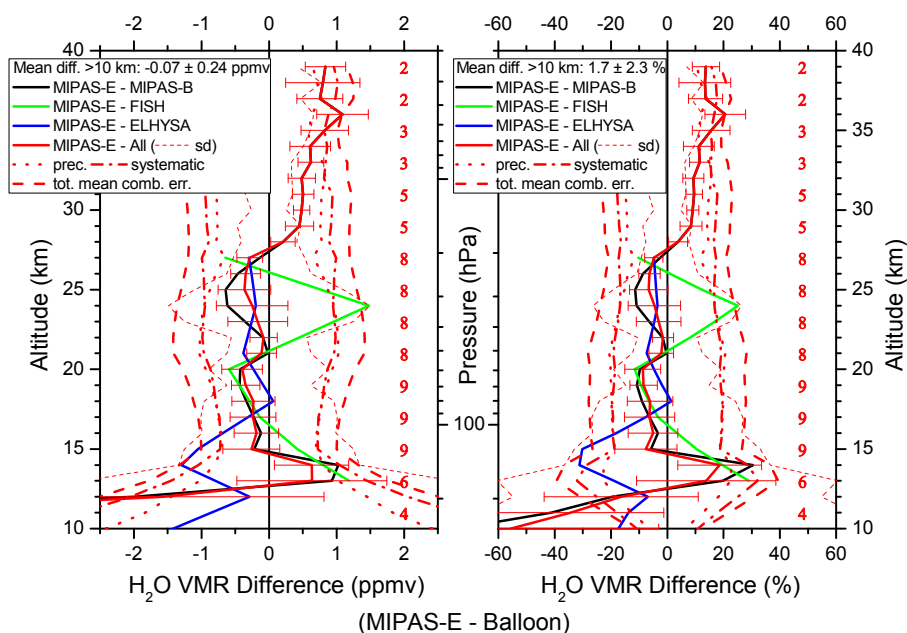


**Fig. 7.** Differences of all (red solid lines) direct comparisons between MIPAS-E and balloon-borne observations of the instruments MIPAS-B (black solid lines), FISH (green solid lines), and ELHYSA (blue solid lines), together with mean combined precision (red dotted lines), systematic (red dash-dotted lines), and total errors (red dashed lines) as well as standard deviation (red thin dotted lines) and the standard error of the mean, plotted as error bars. Red values (along the right-hand y-axes) indicate the number of collocations at corresponding pressure levels.

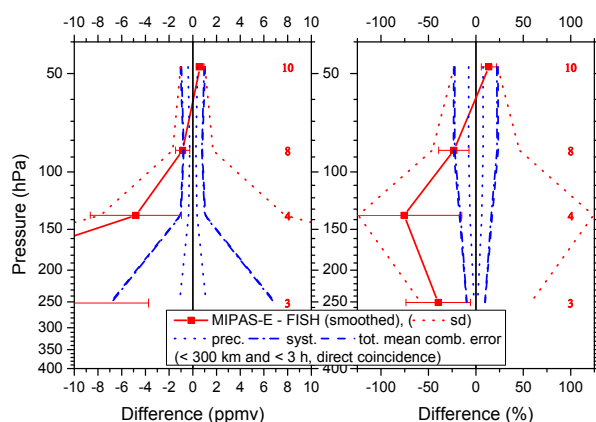


**Fig. 8.** Absolute (left) and relative (right) H<sub>2</sub>O differences (red squared lines) between MIPAS-E and the stratospheric hygrometer FISH for all Geophysica flights carried out above Italy and northern Sweden within a direct coincidence limit of 300 km and 3 h together with mean combined precision (blue dotted lines), systematic (blue dash-dotted lines), and total errors (blue dashed lines) as well as standard deviation (red dotted lines) and the standard error of the mean, plotted as error bars. FISH profiles were smoothed with the averaging kernel of MIPAS-E. Red values (along the right-hand y-axes) indicate the number of collocations at corresponding pressure levels.

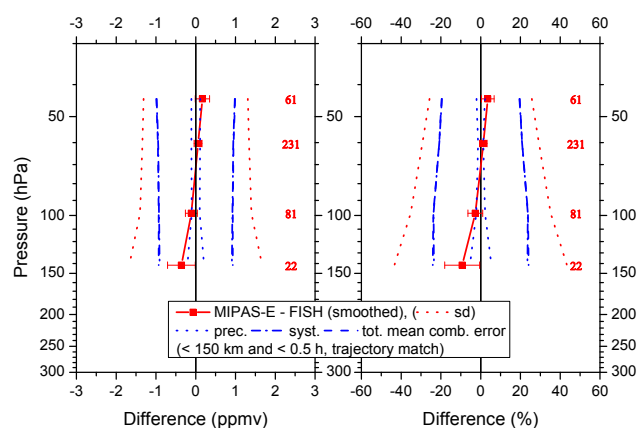


**Fig. 9.** Same as Fig. 8 but for trajectory calculations within a coincidence limit of 150 km and 0.5 h.

likely not influenced by high cirrus. Within this small altitude region in the UT/LS, mean H<sub>2</sub>O VMR differences between MIPAS and smoothed DIAL data are within the combined error bars at the upper edge of the comparable altitude range whereas around the tropopause MIPAS clearly shows a dry bias (Fig. 11).

The Airborne Microwave Stratospheric Observing System (AMSOS) detects spectral emissions of atmospheric water vapour near 183.3 GHz from an aircraft. Two acousto-optical spectrometers resolve the H<sub>2</sub>O line to roughly 1 MHz over

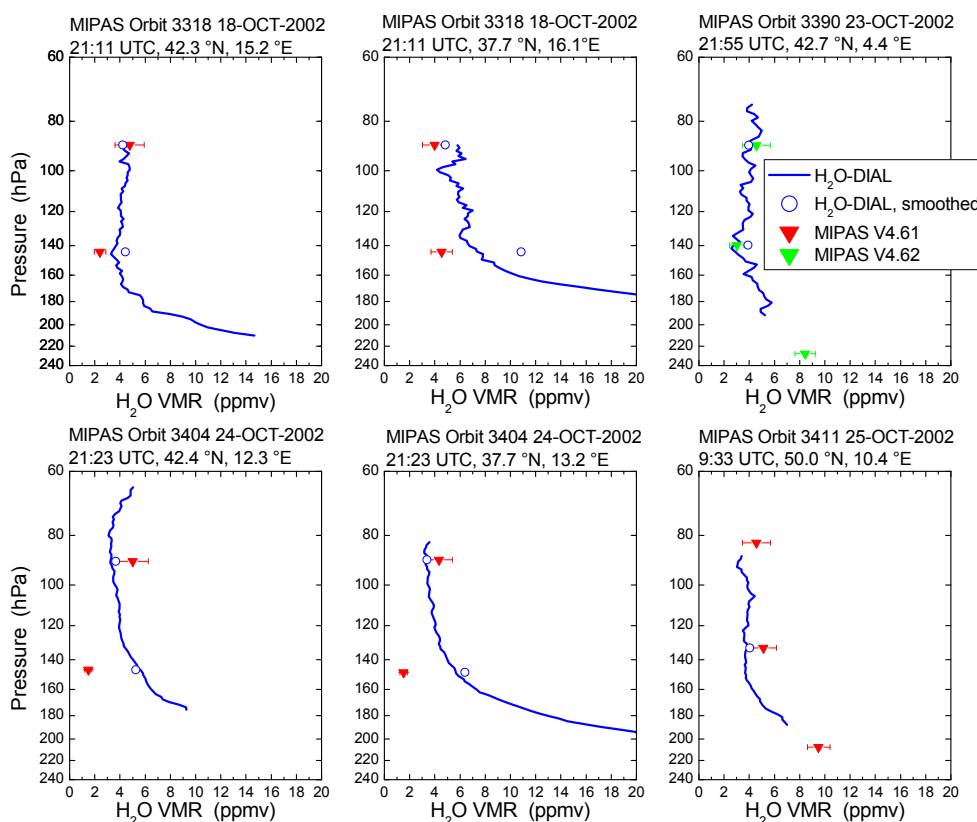


**Fig. 10.** Comparison of observed H<sub>2</sub>O-DIAL profiles (blue solid lines and circles) and MIPAS H<sub>2</sub>O data points version 4.61 (red triangles) and, in one case, version 4.62 (green triangles). H<sub>2</sub>O-DIAL profiles have been smoothed with the averaging kernel of MIPAS.

the whole bandwidth and roughly 25 kHz near the line centre. A single spectrum is measured every 10 to 15 s during the flight. About 20 of them are integrated for improving the signal-to-noise error. From these integrated spectra, altitude profiles of H<sub>2</sub>O VMR between about 15 to 60 km are retrieved along the flight track. A detailed description of the measurement method and instrument is given in Feist et al. (2007) and references therein.

Retrieval method and error analysis are discussed in Müller et al. (2008). ENVISAT validation flights were carried out in September 2002 covering a wide latitude range from the tropics to the Arctic, providing a large number of collocations (Fig. 12). The statistical analysis shows a mean deviation between the data sets in the order of 5 % between 20 and 25 km altitude, increasing to more than 15 % higher up. The mean deviation for all direct collocations found between MIPAS and AMSOS measured H<sub>2</sub>O is positive at all altitudes with values reaching 10 to 20 % above 30 km. This result is in broad agreement with the findings from the balloon comparisons when taking into account that AMSOS data have been assigned with a dry bias of 0–20 % in comparisons to other data sets (cf. Müller et al., 2008).

### 3.3 Intercomparison of satellite observations

Intercomparisons of satellite sensors are useful for cross validation since the large statistics allows identifying potential systematic differences. These are discussed in the following sub-sections. Unless otherwise noted, a standard collocation criterion for maximum space and time separation of 300 km and 3 h between the observations of the two involved sensors has been applied. For each of the selected collocation pairs, both MIPAS and the reference instrument's H<sub>2</sub>O profiles were interpolated to a mean pressure grid over all collocated observations. Since the vertical resolution of H<sub>2</sub>O profiles measured by the validation instruments is comparable to MIPAS no smoothing by averaging kernels has been applied for the intercomparison of the observed profiles.

#### 3.3.1 HALOE comparison

The HALOE instrument was launched in September 1991 on board the UARS satellite and operated until November 2005. The experiment used solar occultation to measure vertical profiles of temperature, O<sub>3</sub>, HCl, HF, CH<sub>4</sub>, H<sub>2</sub>O, NO, NO<sub>2</sub>, and aerosol extinction at four infrared wavelengths (Russell III et al., 1993). The latitudinal coverage ranges from 80° S to 80° N over the course of one year. The channel near

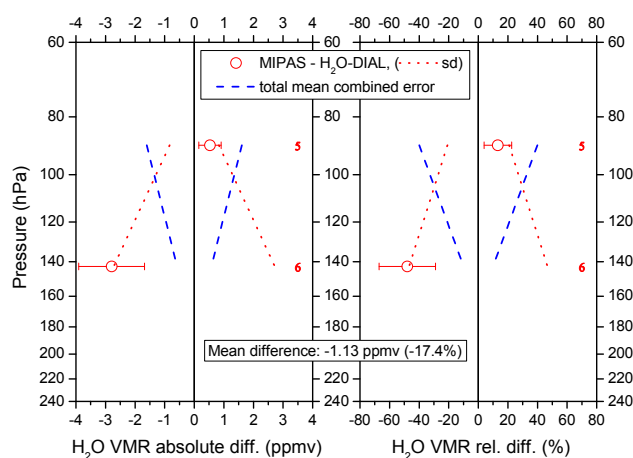


**Fig. 11.** Mean differences of all comparisons between MIPAS and smoothed H<sub>2</sub>O-DIAL observations (red circles) together with mean combined total errors (blue dashed lines) as well as standard deviation (red dotted lines) and the standard error of the mean, plotted as error bars. Red values indicate the number of collocations.

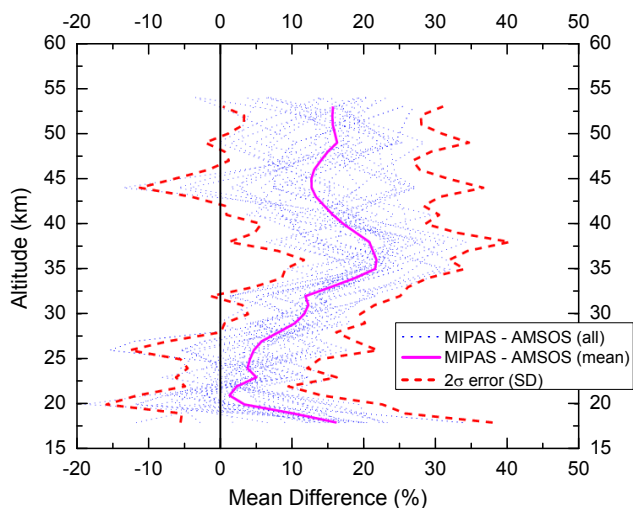


**Fig. 12.** Comparison between MIPAS and AMSOS H<sub>2</sub>O measurements for all available 28 direct collocations (mean difference: magenta solid line). Individual comparisons: blue dotted lines, 2 $\sigma$  standard deviation: red dashed lines.

6.6  $\mu\text{m}$  was tuned to detect the absorption of the H<sub>2</sub>O  $\nu_2$  band. In this study HALOE H<sub>2</sub>O version 19 data are compared to MIPAS. The validation and intercomparison of previous version 17 data (Harries et al., 1996) to independent measurements has shown an overall accuracy of 10 % in the stratosphere and mesosphere (30 % at the upper and lower measurement boundaries). The precision in the lower stratosphere was determined to be within a few percent. According to an intercomparison study of various instruments performed by Kley et al. (2000), HALOE V19 H<sub>2</sub>O data seem to reveal a negative bias of about 5 % in the stratosphere.

Observed differences between MIPAS and HALOE as a function of latitude are given in Fig. 13 and in Table 3. The agreement between both sensors in terms of the mean difference is found to be within a 10 % limit for most coincident altitudes except of the Southern Hemisphere midlatitudes where the deviations are larger in the upper stratosphere. Overall, a general slight positive bias (increasing slightly with altitude) of MIPAS compared to HALOE which extends up to 12 % can be recognized taking into account all collocations (see Fig. 14). Although the observed bias is well within the combined systematic error limits, it is significant in terms of the SEM in the upper stratosphere and lower mesosphere. For all collocations the averaged bias amounts to 7.5 %.

### 3.3.2 SAGE II comparison

The SAGE II experiment on the Earth Radiation Budget Satellite (ERBS) was launched into its non-sun synchronous orbit in October 1984 (Mauldin et al., 1985) and was powered off in August 2005. SAGE II was a seven-channel solar occultation instrument which worked in the visible and near-infrared spectral range. It collected aerosol concentrations and data of trace gases like O<sub>3</sub>, H<sub>2</sub>O, and NO<sub>2</sub> during each sunrise and sunset with a latitudinal coverage between about 80° S and 80° N. H<sub>2</sub>O is retrieved using the 935 nm channel (Chu et al., 1993). In this study, H<sub>2</sub>O data version 6.2 is used for the intercomparison to MIPAS. Precision and accuracy of this data version has been assessed by Taha et al. (2004). In the altitude range between 15 and 40 km, SAGE II H<sub>2</sub>O profiles were reported to show good agreement with correlative measurements within 10 % with a positive bias and decreasing precision above 40 km.

Differences between MIPAS and SAGE II observed H<sub>2</sub>O profiles are displayed in Fig. 15 and in Table 4. Mean deviations between MIPAS and SAGE II are mostly within 10 %, showing a similar behaviour to the HALOE comparison with a positive bias in the MIPAS data. This bias reaches up to 10 % above about 40 hPa when taking into account all collocations and is still clearly within the combined systematic error limit (see Fig. 16). The overall mean deviation between MIPAS and SAGE II is only 5.0 %. Please note that the SAGE II comparisons are confined to a smaller altitude range than the HALOE comparisons.

### 3.3.3 ACE-FTS comparison

The Atmospheric Chemistry Experiment on the SCISAT-1 satellite was launched into its orbit in August 2003 (Bernath et al., 2005). The primary instrument is a high-resolution Fourier transform spectrometer (ACE-FTS) which operates in solar occultation between 750 and 4400  $\text{cm}^{-1}$ . Profiles of a large number of trace species are retrieved from measured spectra with a vertical resolution of 3 to 4 km between about 85° N to 85° S with a majority of observations in the polar

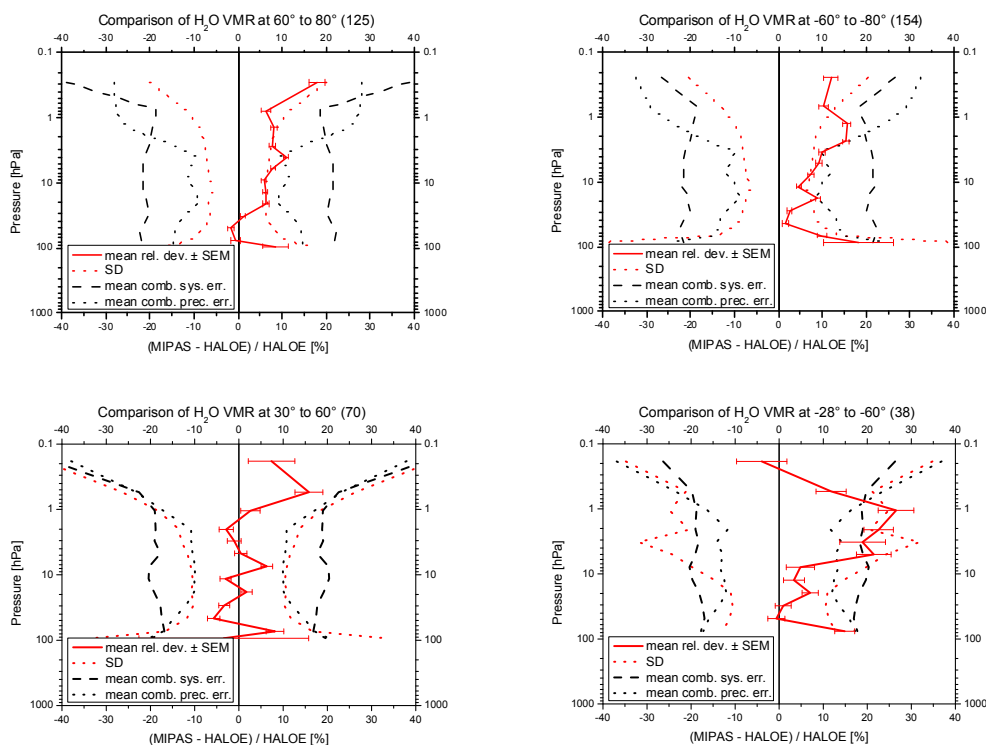


**Fig. 13.** Mean relative deviation (including the standard error of the mean) of H<sub>2</sub>O profiles as measured by MIPAS and HALOE in the Northern (left) and Southern (right) Hemispheres for different latitude regions (red solid lines) from 60–80° N (top left), 30–60° N (bottom left), 28–60° S (bottom right), and 60–80° S (top right). Standard deviation (red dotted lines) and mean combined precision (black dotted lines) and systematic errors (black dashed lines) are also plotted.

**Table 3.** Statistics of the MIPAS vs. HALOE comparison of H<sub>2</sub>O profiles for different latitudinal regions (Zone). Statistical results are given for different pressure altitudes (Press. alt.) and only matches within the same air mass are included; mean relative differences (MRD, (MIPAS-HALOE)/HALOE), standard deviation (SD), and number of collocations (*N*) are also shown.

Zone	Press. alt.	MRD	SD	<i>N</i>	Month of year
60° S–80° S	100–0.2 hPa	2 to 18 %	6–41 %	154	Nov 2002–Jan 2003, Nov 2003–Feb 2004
28° S–60° S	100–0.2 hPa	–4 to 26 %	10–34 %	38	Jan 2003/2004, May 2003, Jul, Aug 2002/2003
30° N–60° N	100–0.2 hPa	–6 to 16 %	10–35 %	70	Jan 2003/2004, Feb 2003, Nov 2003
60° N–80° N	100–0.2 hPa	–1 to 18 %	6–16 %	125	Apr/May 2003, Jul 2002/2003
80° S–80° N	100–0.2 hPa	–1 to 12 %	8–30 %	387	Jul 2002–Feb 2004

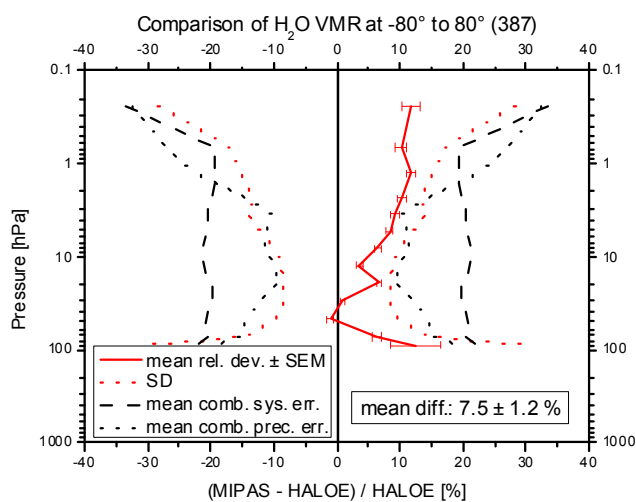
region. H<sub>2</sub>O is one of the key species provided by ACE-FTS. The H<sub>2</sub>O retrieval utilizes numerous microwindows, located in the 950–975 and 1360–2000 cm<sup>–1</sup> spectral regions, to infer profiles from 5 to 90 km altitude. Here we use H<sub>2</sub>O version 2.2 data for the comparison to MIPAS. Profile comparisons of this data version to spaceborne (SAGE II, HALOE, POAM III, MIPAS, SMR) observations and measurements from balloon-borne frost-point hygrometers and a ground-based lidar have been performed by Carleer et al. (2008). The authors show that ACE-FTS measurements provide H<sub>2</sub>O profiles with small retrieval uncertainties in the stratosphere of better than 5 % from 15 to 70 km, gradually increasing above this altitude region. However, a comparison to aircraft H<sub>2</sub>O

observations showed relative differences of about 18 % in the lowermost stratosphere and 30 % in the upper troposphere suggesting a systematic dry bias of the ACE-FTS data, at least for the upper troposphere in winter and spring (Hegglin et al., 2008).

For the MIPAS versus ACE-FTS comparisons the mean difference of all collocations over all latitudes is shown in Fig. 17. For the mean deviation, the agreement between MIPAS and ACE-FTS is quite good over a large altitude region in the stratosphere between about 100 hPa and 0.5 hPa pressure altitude. However, above 0.5 hPa in the mesosphere and below 100 hPa in the region of the upper troposphere and lowermost stratosphere, a dry bias is visible in the

**Table 4.** Same as Table 3 but MIPAS vs. SAGE-II comparison.

Zone	Press. alt.	MRD	SD	<i>N</i>	Month of year
60° S–80° S	100–5 hPa	6 to 11 %	8–16 %	63	Dec 2003, Feb 2004
30° S–60° S	100–5 hPa	2 to 12 %	10–22 %	29	Jan 2003/2004, Apr/May 03, Jul 2003
30° N–60° N	100–5 hPa	–1 to 9 %	8–19 %	27	Jan/Mar/Apr 2003, Jul 2002/2003
60° N–80° N	100–5 hPa	–3 to 9 %	9–18 %	169	Apr/Jun 2003, Jul 2002/2003, Sep 2003
80° S–80° N	100–5 hPa	0 to 9 %	10–17 %	288	Jul 2002–Feb 2004

**Fig. 14.** Mean relative deviation of H<sub>2</sub>O profiles as measured by MIPAS and HALOE for all collocations (387) between 80° S and 80° N. Annotation as per Fig. 13.

MIPAS data. Deviations below 100 hPa are at least partly connected with vertical differences in the altitude position of the tropopause and hygropause in the profiles. Strong H<sub>2</sub>O VMR gradients in the compared profiles can then lead to large differences in the H<sub>2</sub>O values at a specific altitude level. Anyhow, the mean negative bias calculated over all altitudes is only 5.9 %. This, however, goes along with a large standard deviation which exceeds the mean combined precision error.

### 3.4 Intercomparison of ground-based observations and radiosonde data

H<sub>2</sub>O profile observations were carried out within a ground-based measurement campaign for the validation of MIPAS temperature and water vapour data by the Istituto di Metodologie per l'Analisi Ambientale del Consiglio Nazionale delle Ricerche (CNR-IMAA) in Potenza (Italy) and the Department of Physics of the University of L'Aquila (Italy). Radiosondes measuring atmospheric pressure, temperature and relative humidity were launched at the University of L'Aquila (42.4° N, 13.4° E, 683 m above sea level). These profiles were measured with balloon-borne Vaisala RS80 sondes.

For this intercomparison, radiosonde measurements carried out between July 2002 and March 2004 in coincidence with MIPAS overpasses are considered. In accordance with temperature radiosonde vs. MIPAS temperature intercomparisons (Ridolfi et al., 2007), a collocation criterion of 300 km and 3 h was established. Observed profiles have been smoothed with the averaging kernel matrix of MIPAS (above 12 km) to make the altitude resolution of the ground-based measurements comparable to the vertical resolution of the satellite sensor. Below 12 km, a boxcar function smoothing has been applied.

The mean difference of all collocations is displayed in Fig. 18. Differences are mostly within the combined total errors and an overall negative bias of –13.8 % is visible. Strongly increasing H<sub>2</sub>O values below the hygropause lead to larger absolute differences below 12 km (230 hPa) which are somewhat larger than the combined total errors. Above about 30 hPa (24 km) radiosonde data are less reliable, leading to quite large combined errors.

In addition, the CNR-IMAA lidar system for water vapour profiling was used for validation of MIPAS. This lidar instrument is capable of determining, during nighttime, water vapour profiles from about 100 m above the station up to 12 km a.s.l. with high resolution in time and space and with a statistical error typically within 5 % up to 8 km altitude and within 10 % within 8 to 12 km altitude (Mona et al., 2007). For intercomparisons with lidar profiles, the same criterion as for the radiosondes was adopted, but it has to be kept in mind that water vapour lidar profiles are obtained with a temporal integration window (typically 10 minutes) centred around the MIPAS overpass. Therefore lidar and MIPAS observations can be considered as simultaneous.

Lidar profiles of H<sub>2</sub>O were observed from Potenza (40.6° N, 15.7° E) between July 2002 and February 2004. A total of 12 profiles could be used for the comparison which is confined to the narrow overlapping altitude region of both instruments between 5 and 12 km. Results of this comparison are displayed in Fig. 19. A correlation coefficient of  $r = 0.89$  was found. MIPAS underestimates the lidar H<sub>2</sub>O mixing ratios for lidar values below about 20 ppmv, which corresponds to the upper altitudes in the region of intercomparison. Some deviations are at least partly connected with vertical differences in the altitude position of the tropopause and hygropause in the profiles and horizontal inhomogeneities. No

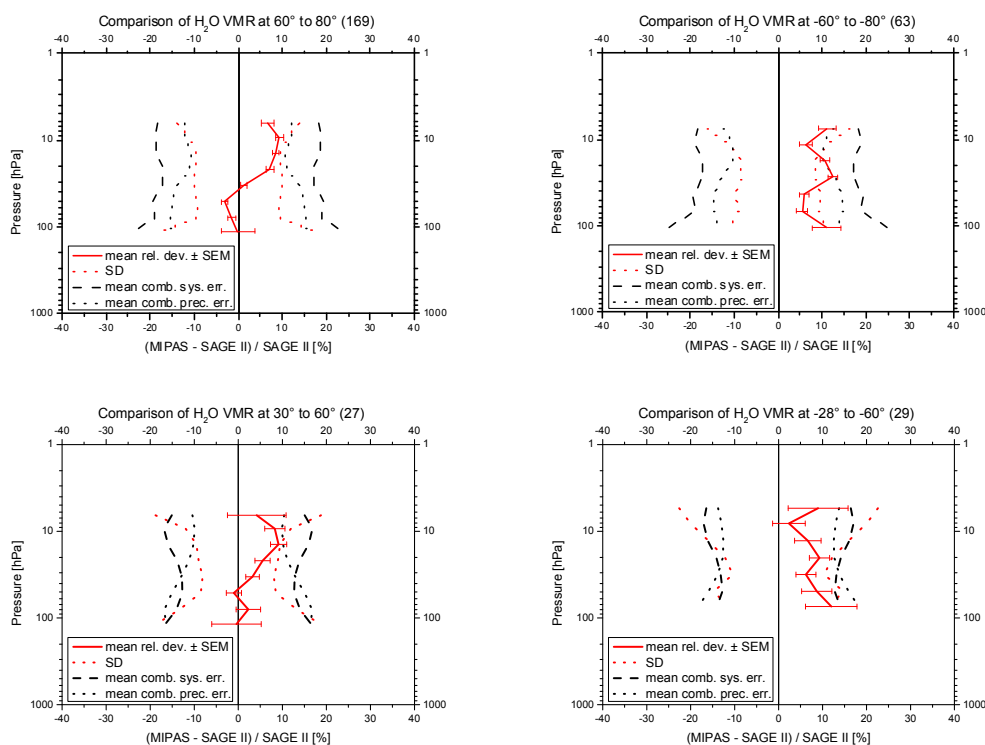


**Fig. 15.** Mean relative deviation (including the standard error of the mean) of H<sub>2</sub>O profiles as measured by MIPAS and SAGE II in the Northern (left) and Southern (right) Hemispheres for different latitude regions from 60–80° N (top left), 30–60° N (bottom left), 28–60° S (bottom right), and 60–80° S (top right). Annotation as per Fig. 13.

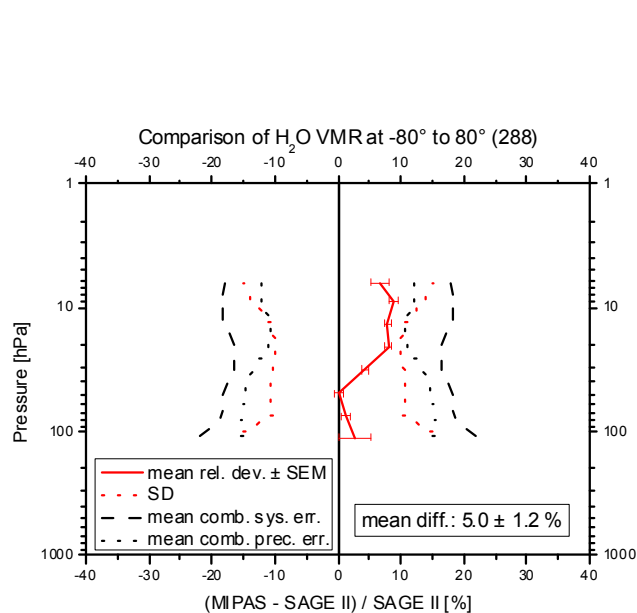


**Fig. 16.** Mean relative deviation of H<sub>2</sub>O profiles as measured by MIPAS and SAGE II for all collocations (288) between 80° S and 80° N. Annotation as per Fig. 13.

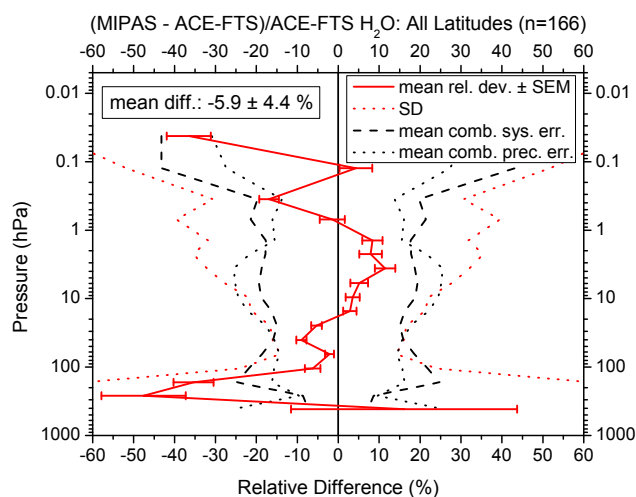


**Fig. 17.** Mean relative difference (including the standard error of the mean) of MIPAS and ACE-FTS H<sub>2</sub>O profiles (166 collocations) between 85° S and 85° N in February and March 2004. Systematic differences appear mainly in the hygropause region below 100 hPa pressure altitude. The standard deviation is exceeding the expected combined precision error over most altitudes. Please note the much broader altitude range as compared to the SAGE-II comparisons. Annotation as per Fig. 13.

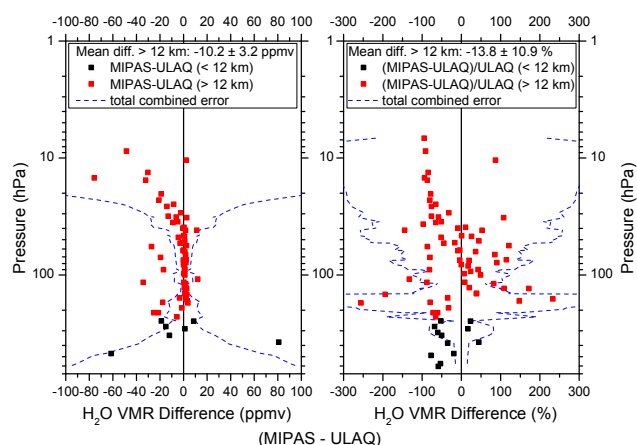


**Fig. 18.** Differences between H<sub>2</sub>O profiles measured by MIPAS and thirteen radio soundings of the University of L'Aquila (smoothed with the MIPAS averaging kernel above 12 km and with a box-car function below 12 km), performed in winter/spring 2002 and 2004, together with combined total errors (blue dashed lines). Black squares: differences below 12 km; red squares: differences above 12 km.

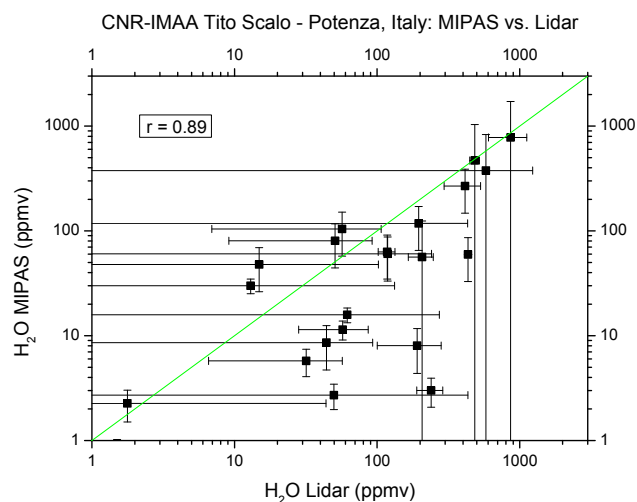


**Fig. 19.** Correlation between H<sub>2</sub>O mixing ratios measured by MIPAS and 12 lidar soundings performed by the CNR-IMAA in Potenza between July 2002 and February 2004. Green line denotes the 1:1 diagonal. A correlation coefficient  $r$  is calculated for all data points.

seasonal dependence between the data of both instruments was observed.

### 3.5 Retrieval processor comparison

MIPAS H<sub>2</sub>O retrieval calculations have also been performed with the dedicated scientific IMK/IAA data processor (von Clarmann et al., 2003) developed at the Institute for Meteorology and Climate Research (IMK) and the Instituto de Astrofísica de Andalucía (IAA). The principal retrieval strategy

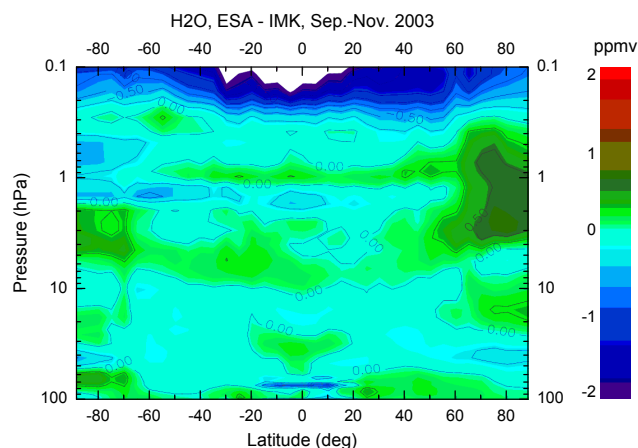


**Fig. 20.** Difference of global zonally averaged H<sub>2</sub>O VMR distributions in the 100 to 0.1 hPa altitude range as retrieved by the ESA and IMK/IAA processors for the September to November 2003 period. Differences are mostly within 0.25 ppmv (or about 10 %) except of the Arctic upper stratosphere and towards the upper boundary of the MIPAS measurement range. Reddish colours denote positive and bluish colours negative deviations.

for H<sub>2</sub>O has been described by Milz et al. (2005). Selected microwindows for the H<sub>2</sub>O retrieval are altitude dependent and are located mainly in the spectral window region between 795 and 960 cm<sup>-1</sup> and in the H<sub>2</sub>O  $\nu_2$ -band between 1220 and 1655 cm<sup>-1</sup>. Since profiles are retrieved on a fine vertical grid (1 km from 6 to 42 km altitude) independent of the actual tangent altitudes, a regularization has been applied to avoid retrieval instabilities.

The zonally averaged H<sub>2</sub>O VMR difference between the distribution retrieved with the processors by ESA and IMK/IAA (data version 13) for a sample period of three months is shown in Fig. 20. Over wide undisturbed regions in the stratosphere between about 100 hPa and 0.5 hPa, the difference between both processors is less than 0.5 ppmv (less than 10 %). Larger differences of more than 1 ppmv occur in the UT/LS region around the tropopause/hygro-pause (not shown in the plot), in the mesosphere, and in the Arctic upper stratosphere. Deviation patterns up to about 0.5 ppmv vary with the season studied. Differences between ESA and IMK/IAA products can arise from the regularization used by IMK/IAA while no regularization has been used by ESA. Furthermore, H<sub>2</sub>O deviations are at least partly connected with differences in the temperature profiles retrieved by the processors. For instance, a temperature difference of 1 K in the stratosphere would result in a H<sub>2</sub>O VMR difference of about 10 %, which corresponds to roughly 0.6 ppmv. Deviations of up to 5 K between the retrieved temperature profiles of both processors occurred, for example, in the mesosphere and upper stratosphere in September 2002 (Wetzel et al., 2007). The comparisons in Fig. 20 have been truncated at 100 hPa, mainly since the IMK/IAA and ESA processors use



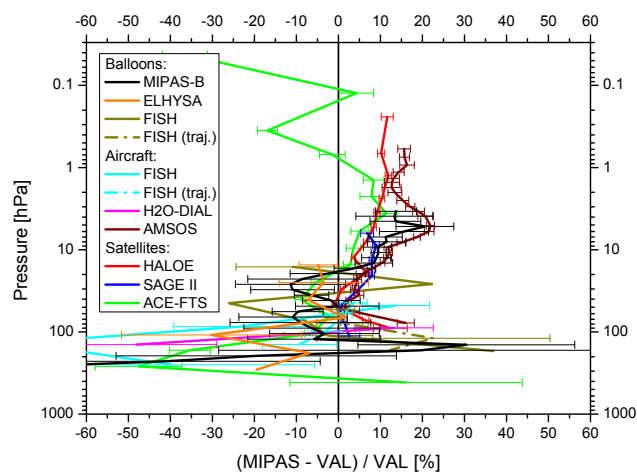


**Fig. 21.** Summary of mean relative (percentage) differences between H<sub>2</sub>O profiles measured by MIPAS and individual satellite, balloon and aircraft validation instruments (VAL) including the standard error of the mean (plotted as error bars) as shown in previous sections. The intercomparison refers to a coincidence criterion of 300 km and 3 h (except for FISH trajectory matches: 150 km, 0.5 h). A clear positive bias of roughly 10 % is visible in the MIPAS data above about 10 hPa pressure altitude. Ground-based and radiosonde comparisons have been omitted for clarity.

different thresholds of the cloud index yielding to different lowermost boundaries of the retrievals.

As shown in various retrieval studies and statistical analyses, H<sub>2</sub>O retrievals may react sensitively to clouds in the FOV, not only at the cloud-affected tangent limb view but also on two (cloud-free) layers above that (e.g. Sembhi H., “Observing water vapour and ozone in the tropical UT/LS with the MIPAS instrument on ENVISAT”, University of Leicester Thesis, 2007). From that, it appears that using a more stringent cloud filtering can reduce some of the variability but does not explain all of the low H<sub>2</sub>O values near the tropopause.

#### 4 Conclusions

The objective of this study has been to validate MIPAS operational H<sub>2</sub>O profiles obtained in the first MIPAS operational period July 2002 to March 2004 (so-called full resolution measurements) by comparison to independent measurements of different previously validated instruments. MIPAS H<sub>2</sub>O vertical profiles have been compared to ground-based, aircraft, balloon-borne, and satellite observations. A retrieval processor comparison has also been included to better assess potential inaccuracies during the operational retrieval procedure. A summary of the assessment of the individual comparisons is given in Table 5 and Fig. 21.

In the lower and middle stratosphere between about 120 and 10 hPa or 15 and 30 km (above the hygropause), ob-

served differences between MIPAS and the validation instruments are mostly well within the combined total error bars. There is no indication of a clear bias in the MIPAS H<sub>2</sub>O profiles in this altitude region.

In the middle and upper stratosphere (above about 15–10 hPa or 28–30 km), a tendency towards a positive bias that is increasing with altitude (up to about 10 %) in the MIPAS satellite and MIPAS-B comparisons can be recognized, which is significant with respect to the standard error of the mean though being mostly within the combined total errors. In addition, the comparison in the hydrogen budget looks very similar. This wet bias in MIPAS H<sub>2</sub>O is also obvious in the AMSOS aircraft comparisons and the satellite comparisons to HALOE, SAGE II, and ACE-FTS. In the mesosphere, the picture is unclear since the satellite comparisons to HALOE and ACE-FTS exhibit different biases.

A critical altitude range for evaluating the validation results is the region of the upper troposphere and lowermost stratosphere (around the tropopause/hygropause). This altitude region is certainly the most challenging for any satellite sensor due to (1) strong spatial gradients in temperature and H<sub>2</sub>O VMR, (2) large horizontal inhomogeneities, (3) FOV effects caused by improper assumptions of the atmospheric state parameters below the lowermost tangent altitude, and (4) straylight and other effects from (thin) cirrus clouds that are not identified in the cloud screening procedures. These effects may on one hand deteriorate the retrievals, on the other hand they undermine the value of conclusions drawn from single comparisons or those with limited statistics. In the comparisons the quality of agreement may be highly dependent on the exact determination of the tropopause and hygropause which marks the sign change in the temperature and H<sub>2</sub>O gradient. Any vertical altitude shift results in comparably large deviations and biases of the intercompared H<sub>2</sub>O profiles in the lowermost stratosphere and upper troposphere. It should be mentioned that single MIPAS H<sub>2</sub>O profiles tend to exhibit retrieval oscillations, particularly in the region of the tropopause/hygropause. This yields, of course, to some larger deviations for specific data points in the compared profiles and to increased standard deviations in statistical comparisons.

The validation results are generally in line with the ex ante estimated MIPAS error limits, particularly within a broad range of the stratosphere. The total MIPAS H<sub>2</sub>O mean retrieval error (accuracy) had been predicted to be within 10 to 30 % in the stratosphere and upper troposphere, with largest errors near the hygropause (Raspollini et al., 2006). The estimation for the random part of the error (precision) typically ranged from 5 to 25 %. Some systematic mixing ratio profile deviations in the validation exercise might also be related to spectroscopy, since different spectral regions were used to derive H<sub>2</sub>O data from observations of different instruments.

Altogether, it can be concluded that MIPAS V4.61 H<sub>2</sub>O profiles collected between July 2002 and January 2004 (so called full resolution data) yield valuable information on

**Table 5.** Quality of the agreement between MIPAS H<sub>2</sub>O data and independent observations carried out by different instruments (coincidence criterion: 300 km and 3h). Time periods, latitudinal regions, and approximate altitudes of the intercomparisons together with comments are summarized.

Instrument	Time period	Latitude region	Approx. alt.	Comments
Balloon comparisons (cf. Figs. 1–7)				
MIPAS-B	Sep 2002/Mar/Jul 2003	NH mid/high	10–39 km	small positive bias >27 km, mean deviation within 20 % above hygropause
ELHYSA	Jan 2003/Mar 2004	NH high	10–27 km	mean deviation within 30 %, small negative bias in Jan 2003
FISH	Mar/Jun 2003	NH high	13–27 km	mean deviation within 20 % (trajectory match) and 30 % (direct comparison)
Aircraft comparisons (cf. Figs. 8–12)				
FISH	Jul/Oct 2002, Jan/Feb/Mar 2003	NH mid/high	9–20 km	negative bias in tropopause region, trajectory comparison within 10 %
H <sub>2</sub> O-DIAL	Oct 2002	NH mid	12–17 km	some negative deviations near 140 hPa
AMSOS	Sep 2002	NH low/mid/high	18–53 km	positive bias above about 30 km, increasing with altitude (up to 20 %)
Satellite comparisons (cf. Figs. 13–17)				
HALOE	Jul 2002–Feb 2004	NH/SH mid/high	16–60 km	mean relative difference: –2 to 12 %, positive bias (except around 50 hPa)
SAGE II	Jul 2002–Feb 2004	NH/SH mid/high	16–36 km	mean relative difference: –1 to 9 %; positive bias above about 30 km
ACE-FTS	Feb/Mar 2004	NH/SH all	7–70 km	mean relative difference: –5.9 %, larger deviations around hygropause and in lower mesosphere, standard deviation generally exceeding combined precision errors
IMK/IAA vs. ESA	Processor versions Sep/Oct/Nov 2003	(cf. Fig. 20) NH/SH all	15–65 km	differences within 10 %, except Arctic upper stratosphere and mesosphere
Ground-based & radiosonde comparisons (cf. Figs. 18–19)				
ULAQ L' Aquila (radiosondes)	Feb 2003–Mar 2004	NH mid	6–23 km	no significant bias, mean deviation small but large standard deviation observed
IMAA Potenza (lidar)	Jul 2002–Feb 2004	NH mid/high	5–12 km	good correlation between both instruments within (large) error bars, no seasonal dependence

global distribution of H<sub>2</sub>O in the stratosphere such that these data sets are very valuable for scientific studies. In the mesosphere, MIPAS errors generally increase and the total error exceeds the 100 % limit above 65 km (Raspollini et al., 2006) such that MIPAS operational data are therefore less reliable above the stratopause. Dedicated codes taking into account non-LTE effects might be advantageous there.

*Acknowledgements.* Financial support by the DLR (Project 50EE0020) and ESA for the MIPAS-B balloon flights is gratefully acknowledged. We thank the Centre National d'Etudes Spatiales (CNES) balloon launching team and the Swedish Space Corporation (SSC) Esrange people for excellent balloon operations, the DLR flight department and the Russian Geophysica crew for excellent campaign operation and the Free University of

Berlin (K. Grunow and B. Naujokat) for meteorological support and trajectory calculations. Assistance by C. Kiemle (DLR) in retrieving the DIAL data is greatly acknowledged. Funding for the ACE mission was provided primarily by the Canadian Space Agency (CSA) and the Natural Sciences and Engineering Research Council (NSERC) of Canada. The authors would like to thank K. Walker, P. Bernath and C. Boone for providing ACE data. We thank the HALOE group at Hampton University, especially to J. M. Russell III, and at NASA LaRC, especially to E. Thompson, and the SAGE II group at NASA LaRC, especially to Larry Thomason, and the NASA Radiation and Aerosol Branch for providing the data and information on these data. The validation work by IUP-IFE Bremen was funded in part by BMBF (FKZ 01 SF994) and ESA/ESRIN under the SciLoV project. The CNR-IMAA ground-based facility for Earth Observation was partly funded by PON 2000–2006, Misura II.1, MIUR. The CNR-IMAA ENVISAT

calibration/validation activities were supported by ESA/ESTEC contract No. 16040/02/NL/SF. The financial support received from Italian “Ministero dell’Ambiente e della Tutela del Territorio e del Mare” for the CETEMPS balloon sounding activities, is gratefully acknowledged. An acknowledgement goes to the work performed by the Quality Working Group established by ESA for verification and monitoring of MIPAS products. We are deeply saddened by the loss of our dear friend and colleague, Cornelius Schiller, who passed away on 3 March 2012. We acknowledge support by Deutsche Forschungsgemeinschaft and Open Access Publishing Fund of Karlsruhe Institute of Technology.

The service charges for this open access publication have been covered by a Research Centre of the Helmholtz Association.

Edited by: W. Lahoz

## References

- Abbas, M. M., Michelsen, H. A., Gunson, M. R., Abrams, M. C., Newchurch, M. J., Salawitch, R. J., Chang, A. Y., Goldman, A., Irion, F. W., Manney, G. L., Moyer, E. J., Nagaraju, R., Rinsland, C. P., Stiller, G. P., and Zander, R.: Seasonal variations of water vapor in the lower stratosphere inferred from ATMOS/ATLAS-3 measurements of H<sub>2</sub>O and CH<sub>4</sub>, *Geophys. Res. Lett.*, 23, 2401–2404, 1996a.
- Abbas, M. M., Gunson, M. R., Newchurch, M. J., Michelsen, H. A., Salawitch, R. J., Allen, M., Abrams, M. C., Chang, A. Y., Goldman, A., Irion, F. W., Moyer, E. J., Nagaraju, R., Rinsland, C. P., Stiller, G. P., and Zander, R.: The hydrogen budget of the stratosphere inferred from ATMOS measurements of H<sub>2</sub>O and CH<sub>4</sub>, *Geophys. Res. Lett.*, 23, 2405–2408, 1996b.
- Bernath, P. F., McElroy, C. T., Abrams, M. C., Boone, C. D., Butler, M., Camy-Peyret, C., Carleer, M., Clerbaux, C., Coheur, P.-F., Colin, R., DeCola, P., De Mazière, M., Drummond, J. R., Dufour, D., Evans, W. F. J., Fast, H., Fussen, D., Gilbert, K., Jennings, D. E., Llewellyn, E. J., Lowe, R. P., Mahieu, E., McConnell, J. C., McHugh, M., McLeod, S. D., Michaud, R., Midwinter, C., Nassar, R., Nichitiu, F., Nowlan, C., Rinsland, C. P., Rochon, Y. J., Rowlands, N., Semeniuk, K., Simon, P., Skelton, R., Sloan, J. J., Soucy, M.-A., Strong, K., Tremblay, P., Turnbull, D., Walker, K. A., Walkty, I., Wardle, D. A., Wehrle, V., Zander, R., and Zou, J.: Atmospheric Chemistry Experiment (ACE): Mission Overview, *Geophys. Res. Lett.*, 32, L15S01, doi:10.1029/2005GL022386, 2005.
- Bertaux, J. L., Mégie, G., Widemann, T., Chassefière, E., Pellinen, R., Korylla, E., Korpela, S., and Simon, P.: Monitoring of ozone trend by stellar occultations: The GOMOS Instrument, *Adv. Space Res.*, 11, 237–242, 1991.
- Bovensmann, H., Burrows, J. P., Buchwitz, M., Frerick, J., Noël, S., Rozanov, V. V., Chance, K. V., and Goede, A. H. P.: SCIAMACHY - Mission objectives and measurement modes, *J. Atmos. Sci.*, 56, 125–150, 1999.
- Brasseur, G., and Solomon, S.: *Aeronomy of the middle atmosphere* (third edition), Atmos. Oceanograph. Sci. Lib., 336 pp., Springer, Dordrecht, the Netherlands, 2005.
- Carleer, M. R., Boone, C. D., Walker, K. A., Bernath, P. F., Strong, K., Sica, R. J., Randall, C. E., Vömel, H., Kar, J., Höpfner, M., Milz, M., von Clarmann, T., Kivi, R., Valverde-Canossa, J., Sioris, C. E., Izawa, M. R. M., Dupuy, E., McElroy, C. T., Drummond, J. R., Nowlan, C. R., Zou, J., Nichitiu, F., Losow, S., Urban, J., Murtagh, D., and Dufour, D. G.: Validation of water vapour profiles from the Atmospheric Chemistry Experiment (ACE), *Atmos. Chem. Phys. Discuss.*, 8, 4499–4559, doi:10.5194/acpd-8-4499-2008, 2008.
- Chiou, E. W., McCormick, M. P., and Chu, W. P.: Global water vapor distributions in the stratosphere and upper troposphere derived from 5.5 years of SAGE II observations (1986–1991), *J. Geophys. Res.*, 102, 19105–19118, 1997.
- Chu, W. P., Chiou, E. W., Larsen, J. C., Thomason, L. W., Rind, D., Buglia, J. J., Oltmans, S., McCormick, M. P., and McMaster, L. R.: Algorithms and sensitivity analyses for SAGE II water vapour retrieval, *J. Geophys. Res.*, 98, 4857–4866, 1993.
- Cortesi, U., Lambert, J. C., De Clercq, C., Bianchini, G., Blumenstock, T., Bracher, A., Castelli, E., Catoire, V., Chance, K. V., De Mazière, M., Demoulin, P., Godin-Beekmann, S., Jones, N., Jucks, K., Keim, C., Kerzenmacher, T., Kuellmann, H., Kuttipurath, J., Iarlori, M., Liu, G. Y., Liu, Y., McDermid, I. S., Meijer, Y. J., Mencaraglia, F., Mikuteit, S., Oelhaf, H., Piccolo, C., Pirre, M., Raspollini, P., Ravegnani, F., Reburn, W. J., Redaelli, G., Remedios, J. J., Sembhi, H., Smale, D., Steck, T., Tadei, A., Varotsos, C., Vigouroux, C., Waterfall, A., Wetzel, G., and Woodet, S.: Geophysical validation of MIPAS-ENVISAT operational ozone data, *Atmos. Chem. Phys.*, 7, 4807–4867, doi:10.5194/acp-7-4807-2007, 2007.
- Engel, A., Schiller, C., Schmidt, U., Borchers, R., Ovarlez, H., and Ovarlez, J.: The total hydrogen budget in the Arctic winter stratosphere during the European Arctic Stratospheric Ozone Experiment, *J. Geophys. Res.*, 101, 14495–14503, 1996.
- Feist, D. G., Geer, A. J., Müller, S., and Kämpfer, N.: Middle atmosphere water vapour and dynamical features in aircraft measurements and ECMWF analyses, *Atmos. Chem. Phys.*, 7, 5291–5307, doi:10.5194/acp-7-5291-2007, 2007.
- Fischer, H., Gille, J., and Russell, J.: Water vapour in the stratosphere: preliminary results of the LIMS experiment aboard Nimbus-7, *Adv. Space Res.*, 1, 279–281, 1981.
- Fischer, H., Birk, M., Blom, C., Carli, B., Carlotti, M., von Clarmann, T., Delbouille, L., Dudhia, A., Ehhalt, D., Endemann, M., Flaud, J. M., Gessner, R., Kleinert, A., Koopmann, R., Langen, J., López-Puertas, M., Mosner, P., Nett, H., Oelhaf, H., Peron, G., Remedios, J., Ridolfi, M., Stiller, G., and Zander, R.: MIPAS: an instrument for atmospheric and climate research, *Atmos. Chem. Phys.*, 8, 2151–2188, doi:10.5194/acpd-8-2151-2008, 2008.
- Flaud, J.-M., Piccolo, C., Carli, B., Perrin, A., Coudert, L. H., Teffo, J.-L., and Brown, L. R.: Molecular line parameters for the MIPAS (Michelson Interferometer for Passive Atmospheric Sounding) experiment, *J. Atmos. Ocean. Opt.*, 16, 172–182, 2003.
- Forster, P. M. D. F. and Shine, K. P.: Stratospheric water vapour changes as a possible contributor to observed stratospheric cooling, *Geophys. Res. Lett.*, 26, 3309–3312, 1999.
- Friedl-Vallon, F., Maucher, G., Seefeldner, M., Trieschmann, O., Kleinert, A., Lengel, A., Keim, C., Oelhaf, H., and Fischer, H.: Design and characterization of the balloon-borne Michelson Interferometer for Passive Atmospheric Sounding (MIPAS-B2), *Appl. Opt.*, 43, 3335–3355, 2004.

- Fueglistaler, S.: Stepwise changes in stratospheric water vapour?, *J. Geophys. Res.*, 117, D13302, doi:10.1029/2012JD017582, 2012.
- Fueglistaler, S., Dessler, A. E., Dunkerton, T. J., Folkins, I., Fu, Q., and Mote, P. W.: The tropical tropopause layer, *Rev. Geophys.*, 47, RG1004, doi:10.1029/2008RG000267, 2009.
- Goss-Custard, M., Remedios, J. J., Lambert, A., Taylor, F. W., Rodgers, C. D., López-Puertas, M., Zaragoza, G., Gunson, M. R., Suttie, M. R., Harries, J. E., and Russell III, J. M.: Measurements of water vapor distributions by the improved stratospheric and mesospheric sounder: Retrieval and validation, *J. Geophys. Res.*, 101, 9907–9928, doi:10.1029/95JD02032, 1996.
- Griesfeller, A., von Clarmann, T., Griesfeller, J., Höpfner, M., Milz, M., Nakajima, H., Steck, T., Sugita, T., Tanaka, T., and Yokota, T.: Intercomparison of ILAS-II Version 1.4 and Version 2 target parameters with MIPAS-Envisat measurements, *Atmos. Chem. Phys.*, 8, 825–843, doi:10.5194/acp-8-825-2008, 2008.
- Harries, J. E., Russell III, J. M., Tuck, A. F., Gordley, L. L., Purcell, P., Stone, K., Bevilacqua, R. M., Gunson, M., Nedoluha, G., and Traub, W. A.: Validation of measurements of water vapor from the Halogen Occultation Experiment (HALOE), *J. Geophys. Res.*, 101, 10205–10216, 1996.
- Heglin, M. I., Boone, C. D., Manney, G. L., Shepherd, T. G., Walker, K. A., Bernath, P. F., Daffer, W. H., Hoor, P., and Schiller, C.: Validation of ACE-FTS satellite data in the upper troposphere/lower stratosphere (UTLS) using non-coincident measurements, *Atmos. Chem. Phys.*, 8, 1483–1499, doi:10.5194/acp-8-1483-2008, 2008.
- Herman, R. L., Drdla, K., Spackman, J. R., Hurst, D. F., Popp, P. J., Webster, C. R., Romashkin, P. A., Elkins, J. W., Weinstock, E. M., Gandrud, B. W., Toon, G. C., Schoeberl, M. R., Jost, H., Atlas, E. L., and Bui, T. P.: Hydration, dehydration, and the total hydrogen budget of the 1999/2000 winter Arctic stratosphere, *J. Geophys. Res.*, 108, 8320, doi:10.1029/2001JD001257, 2002.
- Höpfner, M., Oelhaf, H., Wetzel, G., Friedl-Vallon, F., Kleinert, A., Lengel, A., Maucher, G., Nordmeyer, H., Glatthor, N., Stiller, G., von Clarmann, T., Fischer, H., Kröger, C., and Deshler, T.: Evidence of scattering of tropospheric radiation by PSCs in mid-IR limb emission spectra: MIPAS-B observations and KOPRA simulations, *Geophys. Res. Lett.*, 29, 1278, doi:10.1029/2001GL014443, 2002.
- Kanzawa, H., Schiller, C., Ovarlez, J., Camy-Peyret, C., Payan, S., Jessek, P., Oelhaf, H., Stowasser, M., Traub, W. A., Jucks, K. W., Johnson, D. G., Toon, G. C., Sen, B., Blavier, J.-F., Park, J. H., Bodeker, G. E., Pan, L. L., Sugita, T., Nakajima, H., Yokota, T., Suzuki, M., Shiotani, M., and Sasano, Y.: Validation and data characteristics of water vapor profiles observed by the Improved Limb Atmospheric Spectrometer (ILAS) and processed with the version 5.20 algorithm, *J. Geophys. Res.*, 107(D24), 8217, doi:10.1029/2001JD000881, 2002. (Correction: *J. Geophys. Res.*, 108, 8218, doi:10.1029/2003JD001601, 2003).
- Kiemle, C., Wirth, M., Fix, A., Ehret, G., Schumann, U., Gardiner, T., Schiller, C., Sitnikov, N., and Stiller, G.: First airborne water vapor lidar measurements in the tropical upper troposphere and mid-latitudes lower stratosphere: accuracy evaluation and intercomparisons with other instruments, *Atmos. Chem. Phys.*, 8, 5245–5261, doi:10.5194/acp-8-5245-2008, 2008.
- Kleinert, A., Aubertin, G., Perron, G., Birk, M., Wagner, G., Hase, F., Nett, H., and Poulin, R.: MIPAS Level 1B algorithms overview: operational processing and characterization, *Atmos. Chem. Phys.*, 7, 1395–1406, doi:10.5194/acp-7-1395-2007, 2007.
- Kley, D., Russell III, J. M., and Phillips, C. (Eds.): SPARC assessment of upper tropospheric and stratospheric water vapour, WCRP 113, WMO/TD-1043, SPARC Rep. 2, World Clim. Res. Program, Geneva, 2000.
- Lumpe, J. D., Bevilacqua, R., Randall, C., Nedoluha, G., Hoppel, K., Russell, J., Harvey, V. L., Schiller, C., Sen, B., Taha, G., Toon, G., and Voemel, H.: Validation of Polar Ozone and Aerosol Measurement (POAM) III version 4 stratospheric water vapour, *J. Geophys. Res.*, 111, D11301, doi:10.1029/2005JD006763, 2006.
- Manney, G. L., Santee, M. L., Livesey, N. J., Froidevaux, L., Read, W. G., Pumphrey, H. C., Waters, J. W., and Pawson, S.: EOS Microwave Limb Sounder observations of the Antarctic polar vortex breakup in 2004, *Geophys. Res. Lett.*, 32, L12811, doi:10.1029/2005GL022823, 2005.
- Mauldin III, L. E., Zaun, N. H., McCormick, M. P., Guy, J. H., and Vaughn, W. R.: Stratospheric Aerosol and Gas Experiment II instruments: A functional description, *Opt. Eng.*, 24, 307–312, 1985.
- McKenna, D. S., Konopka, P., Grooß, J.-U., Günther, G., Müller, R., Spang, R., Offermann, D., and Orsolini, Y.: A new Chemical Lagrangian Model of the Stratosphere (CLaMS) 1. Formulation of advection and mixing, *J. Geophys. Res.*, 107, 4309, doi:10.1029/2000JD000114, 2002.
- Michelsen, H. A., Irion, F. W., Manney, G. L., Toon, G. C., and Gunson, M. R.: Features and trends in ATMOS Version 3 water vapor and methane measurements, *J. Geophys. Res.*, 105, 22713–22724, 2000.
- Milz, M., von Clarmann, T., Fischer, H., Glatthor, N., Grabowski, U., Höpfner, M., Kellmann, S., Kiefer, M., Linden, A., Mengistu Tsidu, G., Steck, T., Stiller, G. P., Funke, B., López-Puertas, M., and Koukouli, M. E.: Water vapor distributions measured with the Michelson Interferometer for Passive Atmospheric Sounding on board Envisat (MIPAS/Envisat), *J. Geophys. Res.*, 110, D24307, doi:10.1029/2005JD005973, 2005.
- Mona, L., Cornacchia, C., D’Amico, G., Di Girolamo, P., Pappalardo, G., Pisani, G., Summa, D., Wang, X., and Cuomo, V.: Characterization of the variability of the humidity and cloud fields as observed from a cluster of ground-based lidar systems, *Q. J. Roy. Meteor. Soc.* 133, 257–271, 2007.
- Müller, S. C., Kämpfer, N., Feist, D. G., Haeferle, A., Milz, M., Sitnikov, N., Schiller, C., Kiemle, C., and Urban, J.: Validation of stratospheric water vapour measurements from the airborne microwave radiometer AMSOS, *Atmos. Chem. Phys.*, 8, 3169–3183, doi:10.5194/acp-8-3169-2008, 2008.
- Nassar, R., Bernath, P. F., Boone, C. D., Gettelman, A., McLeod, S. D., and Rinsland, C. P.: Variability in HDO/H<sub>2</sub>O abundance ratios in the tropical tropopause layer, *J. Geophys. Res.*, 112, D21305, doi:10.1029/2007JD008417, 2007.
- Nedoluha, G. E., Bevilacqua, R. M., Gomez, R. M., Hicks, B. C., Russell III, J. M., and Connor, B. J.: An evaluation of trends in middle atmospheric water vapour as measured by HALOE, WVMS, and POAM, *J. Geophys. Res.*, 108, 4391, doi:10.1029/2002JD003332, 2003.
- Offermann, D., Schaeler, B., Riese, M., Langfermann, M., Jarisch, M., Eidmann, G., Schiller, C., Smit, H. G. J., and Read, W. G.: Water vapor at the tropopause during the CRISTA 2 mission, *J. Geophys. Res.*, 107, 8176, doi:10.1029/2001JD000700, 2002.

- Oltmans, S. J., Vömel, H., Hofmann, D. J., Rosenlof, K. H., and Kley, D.: The increase in stratospheric water vapour from balloon-borne frostpoint hygrometer measurements at Washington, D.C. and Boulder, Colorado, *Geophys. Res. Lett.*, 27, 3453–3456, 2000.
- Ovarlez, J. and Ovarlez, H.: Stratospheric water vapor content evolution during EASOE, *Geophys. Res. Lett.*, 21, 1235–1238, 1994.
- Payan, S., Camy-Peyret, C., Oelhaf, H., Wetzel, G., Maucher, G., Keim, C., Pirre, M., Huret, N., Engel, A., Volk, M. C., Kuellmann, H., Kuttippurath, J., Cortesi, U., Bianchini, G., Mencaraglia, F., Raspollini, P., Redaelli, G., Vigouroux, C., De Mazière, M., Mikuteit, S., Blumenstock, T., Velazco, V., Notholt, J., Mahieu, E., Duchatelet, P., Smale, D., Wood, S., Jones, N., Piccolo, C., Payne, V., Bracher, A., Glatthor, N., Stiller, G., Grunow, K., Jeseck, P., Te, Y., and Butz, A.: Validation of version-4.61 methane and nitrous oxide observed by MIPAS, *Atmos. Chem. Phys.*, 9, 413–442, doi:10.5194/acp-9-413-2009, 2009.
- Poberaj, G., Fix, A., Assion, A., Wirth, M., Kiemle, C., and Ehret, G.: All-solid-state airborne DIAL for water vapour measurements in the tropopause region: System description and assessment of accuracy, *Appl. Phys. B*, 75, 165–172, 2002.
- Pumphrey, H. C., Clark, H. L., and Harwood, R. S.: Lower stratospheric water vapor measured by UARS MLS, *Geophys. Res. Lett.*, 27, 1691–1694, doi:10.1029/1999GL011339, 2000.
- Randel, Wu, F., Voemel, H., Nedoluha, G. E., and Forster, P. M. D.: Decreases in stratospheric water vapor after 2001: links to changes in the tropical tropopause and the Brewer-Dobson circulation, *J. Geophys. Res.* 111, D12312, doi:10.1029/2005JB006744, 2006.
- Raspollini, P., Belotti, C., Burgess, A., Carli, B., Carlotti, M., Ceccherini, S., Dinelli, B. M., Dudhia, A., Flaud, J.-M., Funke, B., Höpfner, M., López-Puertas, M., Payne, V., Piccolo, C., Remedios, J. J., Ridolfi, M., and Spang, R.: MIPAS level 2 operational analysis, *Atmos. Chem. Phys.*, 6, 5605–5630, doi:10.5194/acp-6-5605-2006, 2006.
- Raspollini, P., Carli, B., Carlotti, M., Ceccherini, S., Dehn, A., Dinelli, B. M., Dudhia, A., Flaud, J.-M., López-Puertas, M., Niro, F., Remedios, J. J., Ridolfi, M., Sembhi, H., Sgheri, L., and von Clarmann, T.: Ten years of MIPAS measurements with ESA Level 2 processor V6 – Part I: retrieval algorithm and diagnostics of the products, *Atmos. Meas. Tech. Discuss.*, 6, 461–518, doi:10.5194/amtd-6-461-2013, 2013.
- Ridolfi, M., Blum, U., Carli, B., Catoire, V., Ceccherini, S., Claude, H., De Clercq, C., Fricke, K. H., Friedl-Vallon, F., Iarlori, M., Keckhut, P., Kerridge, B., Lambert, J.-C., Meijer, Y. J., Mona, L., Oelhaf, H., Pappalardo, G., Pirre, M., Rizi, V., Robert, C., Swart, D., von Clarmann, T., Waterfall, A., and Wetzel, G.: Geophysical validation of temperature retrieved by the ESA processor from MIPAS/ENVISAT atmospheric limb-emission measurements, *Atmos. Chem. Phys.*, 7, 4459–4487, doi:10.5194/acp-7-4459-2007, 2007.
- Rodgers, C.: Inverse methods for atmospheric sounding: Theory and practice, World Sci. Pub., River Edge, NJ, USA, 2000.
- Rosenlof, K. H., Chiou, E.-W., Chu, W. P., Johnson, D. G., Kelly, K. K., Michelsen, H. A., Nedoluha, G. E., Remsberg, E. E., Toon, G. C., and McCormick, M. P.: Stratospheric water vapour increases over the past half-century, *Geophys. Res. Lett.*, 28, 1195–1198, 2001.
- Rothman, L. S., Jacquemart, D., Barbe, A., Benner, D. C., Birk, M., Brown, L. R., Carleer, M. R., Chackerian Jr., C., Chance, K., Coudert, L. H., Dana, V., Devi, V. M., Flaud, J.-M., Gamache, R. R., Goldman, A., Hartmann, J.-M., Jucks, K. W., Maki, A. G., Mandin, J.-Y., Massie, S. T., Orphal, J., Perrin, A., Rinsland, C. P., Smith, M. A. H., Tennyson, J., Tolchenov, R. N., Toth, R. A., Vander Auwera, J., Varanasi, P., and Wagner, G.: The HITRAN 2004 molecular spectroscopic database, *J. Quant. Spectrosc. Radiat. Transfer*, 96, 139–204, 2005.
- Russell III, J. M., Gille, J. C., Remsberg, E. E., Gordley, L. L., Bailey, P. L., Fischer, H., Girard, A., Drayson, S. R., Evans, W. F. J., and Harries, J. E.: Validation of water vapor results measured by the Limb Infrared Monitor of the Stratosphere experiment on NIMBUS 7, *J. Geophys. Res.*, 89, 5115–5124, 1984.
- Russell III, J. M., Gordley, L. L., Gordley, J. H., Park, J. H., Drayson, S. R., Hesketh, W. D., Cicerone, R. J., Tuck, A. F., Frederick, J. E., Harries, J. E., and Crutzen, P. J.: The Halogen Occultation Experiment, *J. Geophys. Res.*, 98, 10777–10797, 1993.
- Santee, M. L., Manney, G. L., Livesey, N. J., Froidevaux, L., MacKenzie, I. A., Pumphrey, H. C., Read, W. G., Schwartz, M. J., Waters, J. W., and Harwood, R. S.: Polar processing and development of the 2004 Antarctic ozone hole: First results from MLS on Aura, *Geophys. Res. Lett.*, 32, L12817, doi:10.1029/2005GL022582, 2005.
- Scherer, M., Vömel, H., Fueglistaler, S., Oltmans, S. J., and Staehelin, J.: Trends and variability of midlatitude stratospheric water vapour deduced from the re-evaluated Boulder balloon series and HALOE, *Atmos. Chem. Phys.*, 8, 1391–1402, doi:10.5194/acp-8-1391-2008, 2008.
- Solomon, S., Rosenlof, K. H., Portmann, R. W., Daniel, J. S., Davis, S. M., Sanford, T. J., and Plattner, G.-K.: Contributions of stratospheric water vapor to decadal changes in the rate of global warming, *Science*, 327, 1219–1223, 2010.
- Stiller, G. P., von Clarmann, T., Funke, B., Glatthor, N., Hase, F., Höpfner, M., and Linden, A.: Sensitivity of trace gas abundances retrievals from infrared limb emission spectra to simplifying approximations in radiative transfer modeling, *J. Quant. Spectrosc. Radiat. Transfer*, 72(??), 249–280, 2002.
- Taha, G., Thomason, L. W., and Burton, S. P.: Comparison of Stratospheric Aerosol and Gas Experiment (SAGE) II version 6.2 water vapor with balloon-borne and space-based instruments, *J. Geophys. Res.*, 109, D18313, doi:10.1029/2004JD004859, 2004.
- Urban, J., Lautié, N., Murtagh, D., Eriksson, P., Kasai, Y., Loßow, S., Dupuy, E., de La Noë, J., Frisk, U., Olberg, M., Le Flochmoën, E., and Ricaud, P.: Global observations of middle atmospheric water vapour by the Odin satellite: an overview, *Planet. Space Sci.*, 55, 1093–1102, 2007.
- von Clarmann, T., Glatthor, N., Grabowski, U., Höpfner, M., Kellmann, S., Kiefer, M., Linden, A., Mengistu Tsidu, G., Milz, M., Steck, T., Stiller, G. P., Wang, D. Y., Fischer, H., Funke, B., Gil-López, S., and López-Puertas, M.: Retrieval of temperature and tangent altitude pointing from limb emission spectra recorded from space by the Michelson Interferometer for Passive Atmospheric Sounding (MIPAS), *J. Geophys. Res.*, 108, 4736, doi:10.1029/2003JD003602, 2003.
- Wang, D. Y., Höpfner, M., Blom, C. E., Ward, W. E., Fischer, H., Blumenstock, T., Hase, F., Keim, C., Liu, G. Y., Mikuteit, S., Oelhaf, H., Wetzel, G., Cortesi, U., Mencaraglia, F., Bianchini,

- G., Redaelli, G., Pirre, M., Catoire, V., Huret, N., Vigouroux, C., De Mazière, M., Mahieu, E., Demoulin, P., Wood, S., Smale, D., Jones, N., Nakajima, H., Sugita, T., Urban, J., Murtagh, D., Boone, C. D., Bernath, P. F., Walker, K. A., Kuttippurath, J., Kleinböhl, A., Toon, G., and Piccolo, C.: Validation of MIPAS HNO<sub>3</sub> operational data, *Atmos. Chem. Phys.*, 7, 4905–4934, doi:10.5194/acp-7-4905-2007, 2007.
- Wetzel, G., Oelhaf, H., Friedl-Vallon, F., Kleinert, A., Lengel, A., Maucher, G., Nordmeyer, H., Ruhnke, R., Nakajima, H., Sasano, Y., Sugita, T., and Yokota, T.: Intercomparison and validation of ILAS-II version 1.4 target parameters with MIPAS-B measurements, *J. Geophys. Res.*, 111, D11S06, doi:10.1029/2005JD006287, 2006.
- Wetzel, G., Bracher, A., Funke, B., Goutail, F., Hendrick, F., Lambert, J.-C., Mikuteit, S., Piccolo, C., Pirre, M., Bazureau, A., Belotti, C., Blumenstock, T., De Mazière, M., Fischer, H., Huret, N., Ionov, D., López-Puertas, M., Maucher, G., Oelhaf, H., Pommereau, J.-P., Ruhnke, R., Sinnhuber, M., Stiller, G., Van Roozendaal, M., and Zhang, G.: Validation of MIPAS-ENVISAT NO<sub>2</sub> operational data, *Atmos. Chem. Phys.*, 7, 3261–3284, doi:10.5194/acp-7-3261-2007, 2007.
- Zöger, M., Afchine, A., Eicke, N., Gerhards, M.-T., Klein, E., McKenna, D. S., Mörschel, U., Schmidt, U., Tan, V., Tuitjer, F., Woyke, T., and Schiller, C: Fast in situ stratospheric hygrometers: A new family of balloon-borne and airborne Lyman  $\alpha$  photofragment fluorescence hygrometers, *J. Geophys. Res.*, 104, 1807–1816, 1999.